Communications Research Centre

LOW CONVERSION LOSS DIODE RING MIXERS WITH FREQUENCY SELECTIVE TERMINATIONS

by

René J. Douville

DEPARTMENT OF COMMUNICATIONS
MINISTÈRE DES COMMUNICATIONS

CRC REPORT NO. 1216

CANADA

OTTAWA, JULY 1971

COMMUNICATIONS RESEARCH CENTRE

COMMUNICATIONS RESEARCH CENTRE
CANADA

LOW CONVERSION LOSS DIODE RING MIXERS WITH FREQUENCY SELECTIVE TERMINATIONS

by

René J. Douville

(National Space Telecommunications Laboratory)

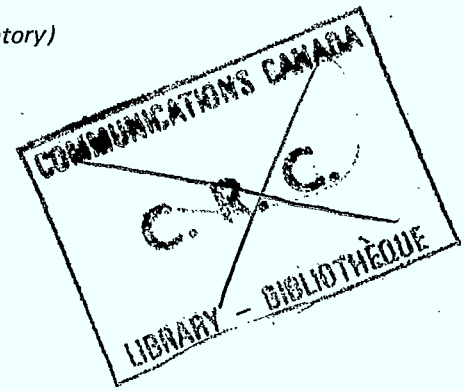

CRC REPORT NO. 1216

Published July 1971
OTTAWA

71-289

TABLE OF CONTENTS

LOW CONVERSION LOSS DIODE RING MIXERS WITH FREQUENCY SELECTIVE TERMINATIONS

by

René Douville

ABSTRACT

The conversion loss of diode ring modulators has been the subject of much investigation. In this report, the special case of a diode ring terminated at its output by a narrowband tuned circuit and at its input by a wideband circuit is investigated. It is shown that the conversion loss of such a system can, in theory, be made arbitrarily small. A system operating at an input frequency range of 50 kHz to 300 kHz and an output frequency of 700 kHz is described and shown to exhibit less conversion loss than that of a resistively terminated diode ring mixer. A similar system designed to operate over an input frequency range of 1 MHz to 20 MHz is then described. It is shown that the performance of this system deviated from the theoretical and in fact, even without selective terminations was able to achieve low conversion loss.

A system is also described which, although not designed specifically to minimize conversion loss, is shown to exhibit low noise figure.

1. INTRODUCTION

The conversion loss of diode ring mixers terminated in various input and output impedance combinations has been investigated for many years. Caruthers[1] as early as 1939 indicated that, by assuming lossless diodes and by terminating the mixer input and output in frequency selective terminations, it was possible to obtain 0 dB power conversion loss. Tucker, in 1949[2] and 1952[3], further elaborated these results and extended them to include the effects of finite forward-and-back diode resistances. For the frequency selective terminations, both Tucker and Caruthers assumed impedances which were either zero or infinite at all unwanted frequencies. Gensel[4] in 1957, and Tucker[5] and Howson and Tucker[6] in 1960, derived results for cases where the terminating impedances are limited to assuming only a finite number of discrete impedance values throughout the entire range of input and output frequencies. In their investigation, Tucker and Howson assumed totally real (or zero or infinite) impedances. Gensel, on the other hand, assumed complex impedances although, in order to render his equations amenable to solution, it is necessary to make simplifying assumptions which severely restrict the usefulness of his techniques. In particular, his technique requires that over the entire range of input and output frequencies, the number of impedance levels which the terminations are permitted to assume is small. Salzmann[7] in 1961, used a similar technique although he made the initial assumption that beyond a certain frequency, the impedances were zero or infinite. In 1964, Kurth[8], using a computer and using the basic techniques of spectral analysis developed by Tucker and elaborated by Gensel, performed an extensive analysis of a ring modulator terminated at the input and output by complex terminations. Due to the limited capabilities of the computer to which he had access, he was required to restrict the range of

frequencies for which finite, non-zero impedances could be considered. With the advent of modern, high capacity computers, this restriction is no longer severe.

Some of the practical problems encountered with the realization of low conversion loss mixer systems by using frequency-selective terminations have been investigated[7,8,9]. However, since the mixer system to be described was, ultimately, to be used in the proposed ISIS-C and possibly in the ISIS-B sounder receiver systems, the problems associated with the development of a wideband input, narrowband output low conversion loss mixer system were of particular interest. In Appendix B, formulas are derived for the conversion loss of such systems. In the analysis, the output impedance of the wideband input terminating network is assumed to be totally reactive at all unwanted input frequencies, while the impedance of the tuned output network is assumed to be zero or infinite at all unwanted output frequencies. It is shown that, under these conditions, it is possible to obtain arbitrarily low mixer system conversion losses.

In Section 2, a system, operating over the input frequency range of 50 to 300 kHz with an output frequency of 700 kHz is described. This is followed, in Section 3, by a description of a mixer system originally designed to operate over the input frequency range 1 to 20 MHz, the expected frequency range of the proposed ISIS-C sounder receiver system. It is shown that the performance of the high frequency system deviated from the theoretical performance and, in fact, even without selective terminations, was able to achieve low conversion loss. The cause of this anomalous behaviour was investigated and the results of that investigation are also reported.

Section 4, although not dealing specifically with low conversion loss mixer systems, does deal with the topic of mixers whose terminations are frequency selective. In particular, a receiver system is described which consists of a diode ring mixer with frequency selective terminations followed by a low noise figure amplifier. It is first shown that such a system should exhibit a very low noise figure and the results of an experimental investigation are then presented.

2. LOW FREQUENCY INVESTIGATION

2.1 NARROWBAND SYSTEM

2.1.1 Review of Theory

The four-terminal equivalent to the ring modulator may be represented as in Figure 1. Here y(t) is the reversible modulating function defined by

$$v_{34} = y(t)v_{12} \longleftrightarrow v_{12} = y(t)v_{34}$$

$$i_{34} = y(t)i_{12} \longleftrightarrow i_{12} = y(t)i_{34}$$

and is given by

$$y(t) = \frac{4}{\pi}(\cos pt - \frac{1}{3}\cos 3pt + \frac{1}{5}\cos 5pt - ....) \qquad .....(1)$$

where p is the local oscillator (LO) or carrier frequency.

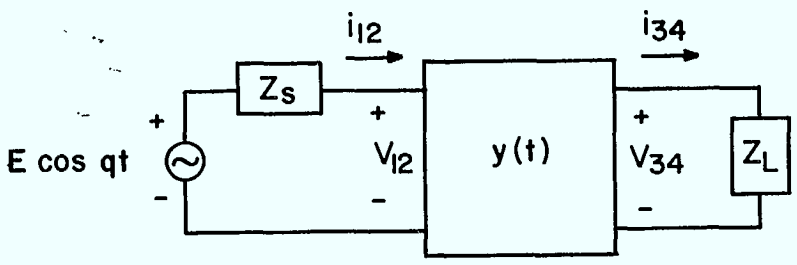

Fig. 1. Four terminal equivalent to the ring modulator circuit.

If the source frequency is q then it is obvious that the output contains components at all frequencies np ± q, n odd while the input contains components at all frequencies mp ± q, m even. Many authors [1-11] have investigated the effects of terminating the input and output of the mixer in a variety of impedance combinations at the various frequency components. Some of the results of their analyses have been compiled and are given in Table 1 in Appendix A. Two cases of particular interest occur for which;

Case 1

$$Z_S = \begin{cases} R_S & f = q \\ 0 & \text{all other frequencies } np \pm q,\ n \text{ even} \end{cases} \qquad \ldots\ldots (2)$$

while

$$Z_L = \begin{cases} R_L & f = p - q \\ \infty & \text{all other frequencies } mp \pm q,\ m \text{ odd} \end{cases}$$

or *Case 2*

$$Z_S = \begin{cases} R_S & f = p - q \\ \infty & \text{all other frequencies } np \pm q,\ n \text{ even} \end{cases} \qquad \ldots\ldots (3)$$

while

$$Z_L = \begin{cases} R_L & f = p - q \\ 0 & \text{all other frequencies } mp \pm q,\ m \text{ odd} \end{cases}$$

and for which it is theoretically possible to obtain zero loss frequency translation. It may be seen that case 1 corresponds to a parallel tuned input and series tuned output while case 2 corresponds to a series tuned input and parallel tuned output. The conversion loss L, defined to be the ratio of the maximum available power to the power delivered to the load at p − q, is given in case 1 by,

$$L = \frac{1}{\pi^2}\frac{R_S}{R_L} + \frac{1}{2} + \frac{\pi^2}{16}\frac{R_L}{R_S} \qquad \ldots\ldots (4)$$

and in case 2 by

$$L = \frac{\pi^2}{16}\frac{R_S}{R_L} + \frac{1}{2} + \frac{1}{\pi^2}\frac{R_L}{R_S} \qquad \ldots\ldots (5)$$

The forward resistance r_d of the diodes is assumed equal to zero and the back resistances of the diodes is assumed to be infinite.*

Equation (4) is minimized for

$$\frac{R_S^2}{R_L^2} = \frac{\pi^4}{16} \qquad \ldots\ldots (6)$$

while equation (5) is minimized for

$$\frac{R_S^2}{R_L^2} = \frac{16}{\pi^4} \qquad \ldots\ldots (7)$$

In both cases, the minimum conversion loss is L = 1.

2.1.2 Development of a Narrowband System

2.1.2.1 General Comments

To verify the above equations, it was decided to build a ring modulator and terminate it in series and parallel tuned circuits as approximations to the conditions given in equations (2) and (3). The three mixer configurations illustrated in Figure 2 were considered. System (a) was eliminated from consideration when preliminary measurements indicated that it would be extremely difficult to obtain transformers capable of transforming the wideband impedance characteristics of frequency selective circuits with any degree of fidelity.† This was mainly a result of the practical difficulties encountered in obtaining a transformer with the high primary inductance required (high with respect to the series tuned inductance) while at the same time maintaining a low shunt capacitance (low with respect to the series tuned capacitance). In certain applications, one of system (b) or (c) may have advantages over the other. However, since no such advantage existed here, it was decided to use configuration (b).

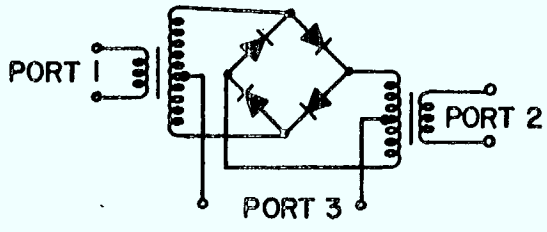

SYSTEM	PORT 1	PORT 2	PORT 3
(a)	SIGNAL	LOAD	L.O.
(b)	L.O.	LOAD	SIGNAL
(c)	SIGNAL	L.O.	LOAD

Fig. 2. Diode Ring Modulator illustrating three mixer configurations.

---

* For modern semiconductor diodes, this assumption is very reasonable since the back resistance may be greater than 100 MΩ while the forward resistance may be lower than 1Ω.

† Gensel[4] mentions this same problem and Salzmann[7] indicates a method of eliminating the problem.

2.1.2.2 Preliminary Investigation

The circuit shown in Figure 3, but without the series turned input and using the following parameter values, was built to isolate and analyze some of the problems to be met:

1. $R_S = 600 - 700\Omega$.
2. Frequencies q → 10 kHz (signal or RF)
   p - q → 20 kHz (IF)
   p → 30 kHz (LO)
3. $R_{LO} = 25,50,100,430\Omega$
4. $V_{LO} = 35v$ p-p
5. T1 (a) 500 μH primary inductance
   (b) 10 mH primary inductance
6. $R_P = 1K\Omega$, $R_L = R_P \parallel r_p$ where R_L is the effective load resistance and r_p is the effective parallel resistance of the tuned transformer
   R_L was determined to be 650Ω
7. $C_1 = 0.1\mu F$ chosen to be as large as possible (for high tuned circuit loaded Q) consistent with a reasonable component Q at 20 kHz.
8. T2 $L_P = 320\mu H$ primary inductance chosen to give p - q (IF) at 20 kHz with C_1.

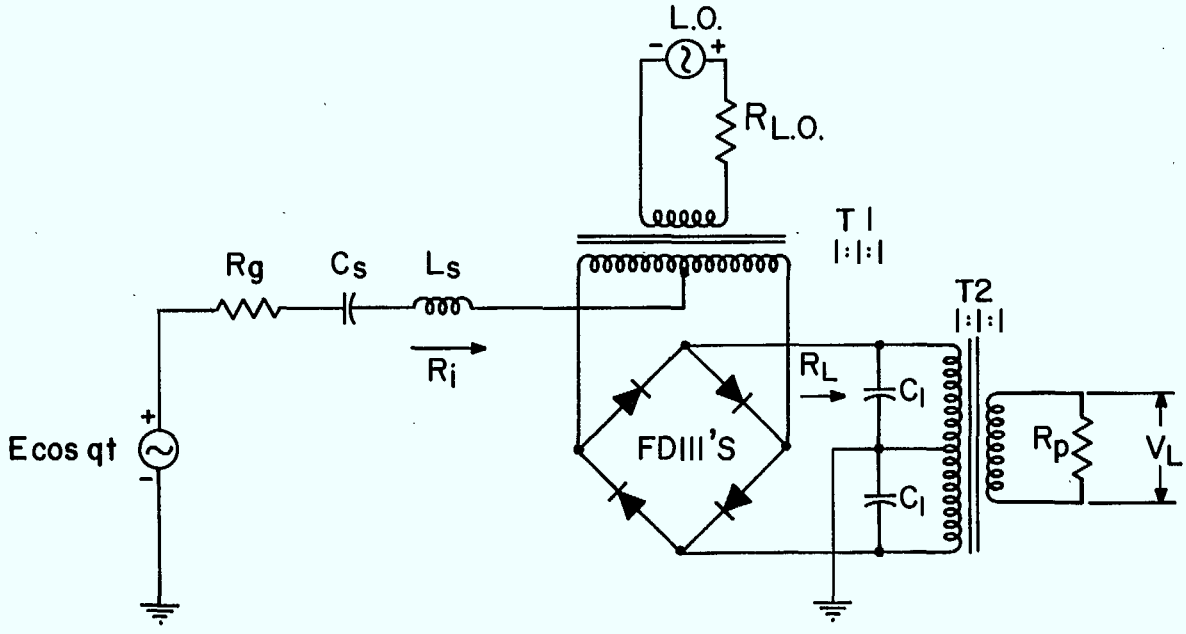

Fig. 3. Narrowband, Low Frequency, Low Conversion Loss, diode ring mixer system.

The resultant operating Q was*

$$Q_{eff} \cong \frac{650 \parallel 650}{X_{L_P}} \cong 8$$

The FD111 diodes were chosen on the basis of high switching speed, high conductance and greater than 250 MA average current capability.

With lv p - p signal input, the output signal level at the upper sideband frequency (p + q → 44 kHz) was found to be approximately 20 dB below the IF at p - q (20 kHz). This distortion, visually noticeable on the output waveform, was approximately that predicted for a Q_{eff} of 8.

For 700 mA peak-to-peak LO drive current from a 100Ω source, a substantial "dead zone" (when the diode ring is open) was seen to occur. Although the duration of this dead zone depended, as expected, primarily on the frequency of operation, some dependence on the primary inductance of T1 and the magnitude of the LO source impedance R_{LO} was also indicated. It was concluded that the magnitude of R_{LO} should be maximized subject to the limitation that the diode current remain large enough to keep the diodes still well into the ON region. Also, the T1 primary inductance should be as large as possible to minimize the magnetizing-current-to-diode-current ratio provided the transformer leakage inductance does not begin to interfere with the switching of the diodes for the particular value of R_{LO} chosen.

2.1.2.3 A Narrowband System

Using the above results as guidelines, the complete circuit shown in Figure 3 was constructed.

A further restriction imposes itself in tuning both the input and the output. The effective Q of the parallel tuned output circuit is given approximately by

$$Q_{peff} = \frac{R_L \parallel \frac{\pi^2}{4} R_S}{(p-q)\, L_p} = \frac{R_L}{2(p-q)\, L_p} = \frac{1}{2}(p-q)\, C_p R_L = (p-q)\, C_1 R_L \qquad \ldots\ldots (8)$$

while that for the series tuned circuit is given by

$$Q_{seff} = \frac{q_{LS}}{R_S + \frac{4}{\pi^2} R_L} = \frac{q_{LS}}{2R_S} = \frac{\pi^2}{8} \frac{qL_S}{R_L} \qquad \ldots\ldots (9)$$

since for the zero conversion loss case $R_S = \frac{4}{\pi^2} R_L$. These Q values are, strictly speaking, restricted only by the magnitudes of available components. In practice, the maximum value of L_S is limited by the effect of stray inductor winding capacitance. Also, the maximum value of C_1 is limited by the deterioration in Q of available capacitors as their values increase. Due therefore to these limitations in L_S and C_1, for any desired frequency of operation, Q_s and Q_p are dependent in inverse ways on R_L. Thus, the choice of R_L is very important in obtaining high working Q's at both the input and the output.

---

* The effective resistance paralleling the output tuned circuit is equal to the load paralleled by the transformed source impedance which in this case is $R \cong R_S$.

In the final circuit, L_S = 95.3 mH with a Q of 200–400 in the frequency range 11 - 50 kHz with a winding capacitance C_o' = 29 pF corresponding to a measured self-resonance of 105 kHz. The operating frequencies p and q were selected to give the following nominal circuit frequencies in order to take advantage of the L_S impedance variations:

Input Signal (RF)	q → 20 kHz	
LO Frequency	p → 52.5 kHz	
Output Signal (IF)	p-q → 32.5 kHz	
Upper Sideband	p+q → 72.5 kHz	
Image	2p-q → 85 kHz	} suppressed by self
Converted Upper Sideband	2p+q → 125 kHz	} resonance of L_S at 105 kHz.

C_S was then chosen as 680 pF. With C_1 = 0.1μF(Q≅200), the primary inductance required at the output transformer was determined, wound and measured to be 126μH, which when resonated with C_1, gave an unloaded Q of 50. With R_p = 5.8 kΩ, the effective load resistance R_L = 1kΩ .

For this value of load resistance, zero conversion loss operation requires that the source resistance R_S be $R_S = \frac{4}{\pi^2} R_L = 405\Omega$. The value of R_S was taken to be equal to the sum of the generator resistance R_g and the effective series loss resistance r_s of the series tuned circuit. R_g was therefore adjusted until the value of R_S = 405Ω was obtained.

The LO transformer T1, was wound to have a primary inductance L_{LO} of 9 mH which is equivalent to restricting the peak LO magnetizing current to less than 10 per cent of the peak diode current. The corresponding leakage inductance was measured to be 16 μH. The LO source impedance was selected to be 1kΩ with the LO level adjusted to give 15 mA zero-to-peak per diode on current (on resistance ≅ 10 Ω).

Once all components were connected, the signal and LO frequencies were tuned to obtain a maximum output. It was found that the input current varied with frequency as indicated in Figure 4.

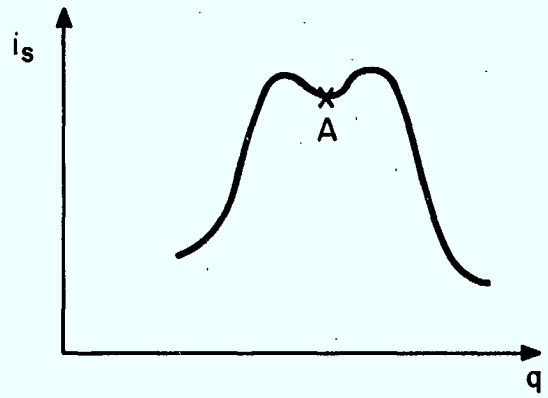

Fig. 4. Variation of input current with signal frequency.

This may be considered to be a result of the amount of coupling which the input and output tuned circuits experience through the mixer. The local minimum (A) was found to coincide with maximum output as well as with the resonant frequency of the series tuned circuit alone.

To check the impedance transforming properties of the mixer, the input impedance R_i of the mixer was measured to be 383Ω. This is equivalent to an $R_L = \frac{\pi^2}{4} \cdot 383\Omega = 946\Omega$ which compares favourably with the actual value of 1kΩ. The conversion loss was then measured to be

$$L = \frac{E^2}{4R_s} \frac{R_L}{V^2}$$

$$= \left(\frac{2.59}{1.83}\right)^2 \frac{1000}{4x405} = 1.24 \rightarrow 0.9 \text{ dB}.$$

It may be argued that, since the series and parallel tuned circuit losses have been included in the source and load resistances, the conversion loss figure quoted is not realistic; in fact the conversion loss in the above case without the loss resistances taken into account was greater than 10 dB. However, since the purpose of the experiment here was to verify the theory, the actual location of the source and load resistances was not of great importance and special pains were not taken to isolate these losses from the tuned circuits.

The above result may be taken as sufficient indication that the theory is indeed correct and that is is possible to terminate ring modulators in frequency selective terminations, to obtain low conversion loss.

2.2 WIDEBAND SYSTEMS

2.2.1 General Comments

Although it has been shown that it is possible to obtain low conversion loss frequency translation in narrowband systems, in many applications a wideband input is desirable. Therefore, the possibility of terminating the input in either a lowpass or broadband bandpass network was investigated.

The low conversion loss theory as developed in the literature assumes either zero or infinite impedances at unwanted frequencies[1,2,5] or alternatively, the impedance is limited to a small number of discrete impedance levels each of which exists over a corresponding range of unwanted frequencies[4,7]. It is therefore very difficult, on the basis of this theory, to predict the effects of finite, continuously varying reactive terminations at these frequencies on the performance of diode ring modulators. As an alternative, the impedances occurring at unwanted frequency components in the narrowband case were used as guidelines in a computer-aided investigation of various lowpass and bandpass impedance characteristics. In general, it was found that the high or low impedance required to satisfy[1,2,5] could not be maintained over the full range of unwanted frequencies (even if that range were limited only to the image frequency at 2p-q) unless the IF was far removed from the highest RF frequencies. In the proposed ISIS-C sounder receiver for which the investigation was instigated, this situation would not be satisfactory since it could result in severe problems with oscillator stability. It was therefore decided to investigate the theory of mixers whose inputs are terminated in impedances which are finite and reactive at unwanted frequency components.

2.2.2 Analytical Investigation and Results

A complete analysis appears in Appendix B and applies to the systems shown in Figure 5. In these systems, it is assumed that the impedances of the series or parallel tuned output circuits are either zero or infinite at frequencies other than the IF. The output impedance of the input filter is limited only by the assumption that it be totally reactive at all unwanted input frequencies. It is also assumed that the diodes have zero forward resistance and infinite back resistance.

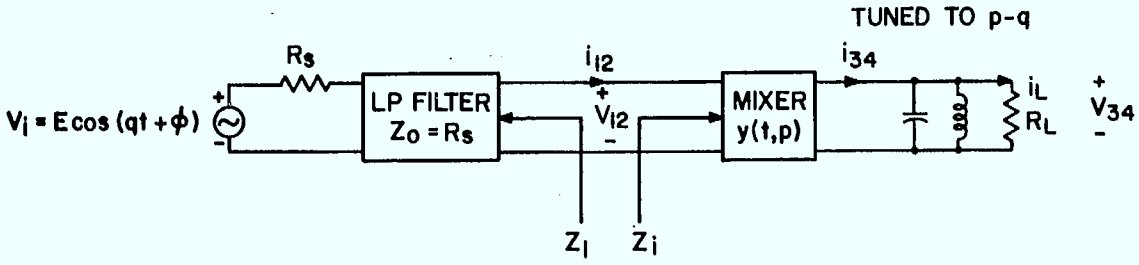

SYSTEM A

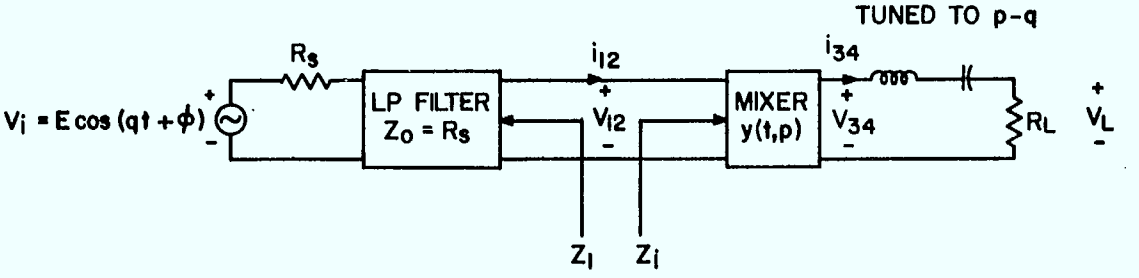

SYSTEM B

Fig. 5. Wideband-input low conversion loss mixer systems.

From the Appendix B, the conversion power loss of system A is given by

$$L = \frac{R_L}{4R_S}\left[\left(\frac{\pi}{2}\frac{R_S}{R_L} + \frac{2}{\pi}\right)^2 + \frac{4R_S^2}{\pi^2 X_{eq}^2}\right] \qquad \ldots\ldots(10)$$

where

$$\frac{1}{X_{eq}} \triangleq \left(\frac{1}{X_{2-}} - \frac{1}{9X_{2+}} + \frac{1}{9X_{4-}} - \frac{1}{25X_{4+}} + \ldots\ldots\right)$$

and for system B

$$L = \frac{R_S}{4R_L}\left[\left(\frac{\pi}{2}\frac{R_L}{R_S} + \frac{2}{\pi}\right)^2 + \frac{4}{\pi^2}\frac{X_{eq}^2}{R_S^2}\right] \qquad \ldots\ldots(11)$$

where

$$X_{eq} \triangleq \left(X_{2-} - \frac{1}{9}X_{2+} + \frac{1}{9}X_{4-} - \frac{1}{25}X_{4+} + \ldots\ldots\right)$$

In these equations R_S is the source impedance equal to the lowpass filter characteristic impedance, R_L is the load impedance and X_{eq}, defined as indicated, represents the effect of the finite reactive impedances at the unwanted frequencies in the stopband of the filter. Equation (10) is minimized for

$$R_{Lmin} = \frac{\pi^2}{4} R_S \left(\frac{X_{eq}}{\sqrt{R_S^2 + X_{eq}^2}} \right) \quad \ldots\ldots (12)$$

and the minimum is given by

$$L_{min} = \frac{1}{2} \left[1 + \frac{\sqrt{R_S^2 + X_{eq}^2}}{X_{eq}} \right] \quad \ldots\ldots (13)$$

Likewise, equation (11) is minimized for

$$R_{Lmin} = \frac{4}{\pi^2} R_S \sqrt{1 + \frac{X_{eq}^2}{R_S^2}} \quad \ldots\ldots (14)$$

and the minimum is given by

$$L_{min} = \frac{1}{2} \left[1 + \sqrt{1 + \frac{X_{eq}^2}{R_S^2}} \right] \quad \ldots\ldots (15)$$

In most practical cases, R_L is made equal to $\frac{\pi^2}{4} R_S$ in system A and $\frac{4}{\pi^2} R_S$ in system B since R_L as specified by equations (12) or (14) is dependent on X_{eq} and is therefore frequency dependent and very difficult to realize. The conversion losses are then given by

$$\text{System A} \quad L = 1 + \frac{1}{4} \frac{R_S^2}{X_{eq}^2} \quad \ldots\ldots (16)$$

and

$$\text{System B} \quad L = 1 + \frac{1}{4} \frac{X_{eq}^2}{R_S^2} \quad \ldots\ldots (17)$$

Equations (13) to (17) inclusive are plotted in Figure 6 and indicate that even for the extreme case when X_{eq} is equal to R_S, the conversion losses are still less than 1 dB or about 3 dB improvement over the resistively terminated case. Typically, X_{eq} is 2 or 3 times R_S for system A and 1/2 to 1/3 of R_S for system B. For completeness, the derivations of the input impedances Z_i of the above systems are also included in Appendix B.

2.2.3 Experimental Investigation and Results

To verify the above results, a mixer system similar to that shown in Figure 10 (page 13) but without the frequency dependent terminations was constructed. The results of section 2.1 were used as guidelines in selecting the component values. However, initial measurements indicated excessivly high losses which further investigation revealed to be a result of excessive interwinding capacitance in transformer T1. This may be illustrated as follows.

The signal transformer may be drawn as in Figure 7 (a) where the effects of transformer inductances and shunt capacitances have been neglected. If the diode ON resistance r_d is assumed to be zero, then the transformer

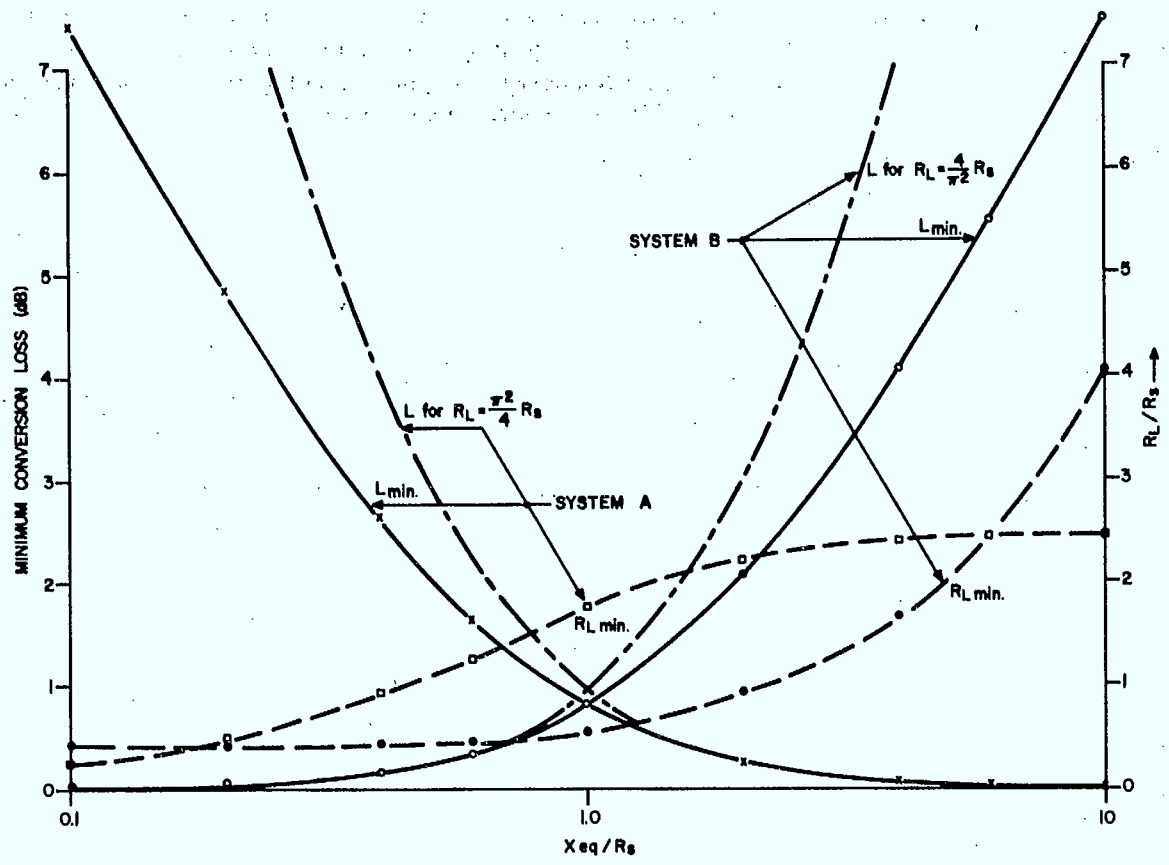

Fig. 6. Minimum conversion loss and required load resistance for mixer with lowpass filtered input and tuned output.

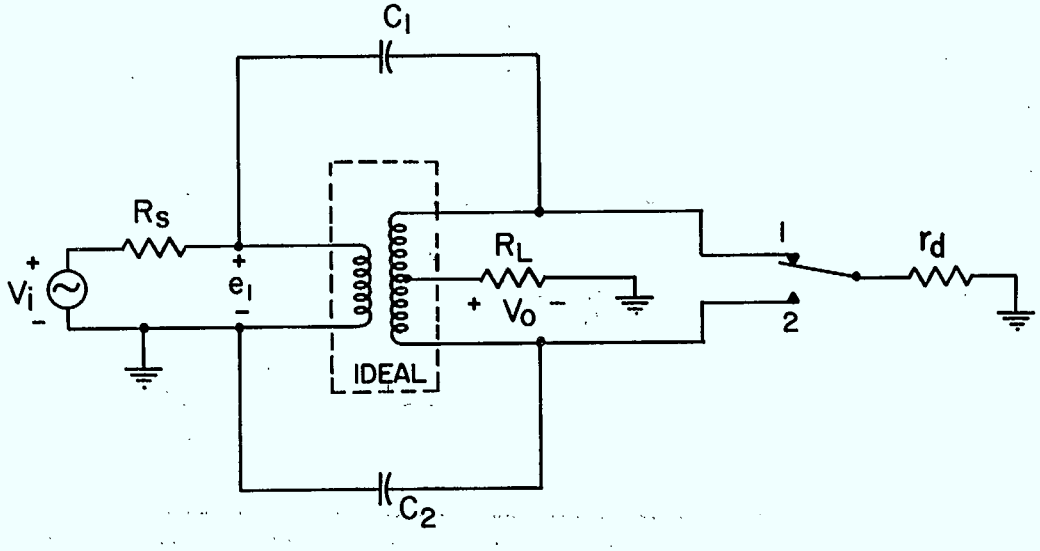

Fig. 7(a). Signal transformer circuit where the diode ring is represented by a reversing switch. The capacitors C_1 and C_2 represent the transformer interwinding capacitance and the remainder of the transformer is assumed ideal.

equivalent circuit appears as in Figure 7, (b) and (c), for the two switch positions. If it is assumed that the switching frequency is much higher than the signal frequency, the circuit output voltage waveform appears as shown in Figure 8*. The time constants of the transients may be obtained from Figure 7, (b) and (c) and are $\tau_1 = (R_S \,//\, R_L)(C_1 + 4C_2)$ and $\tau_2 \simeq (R_S \,//\, R_1)C_1$. For the transformer and circuit used, $C_1 \cong C_2 \cong 70$ pF and $R_S = R_L = 500\ \Omega$ giving $\tau_1 = 87.5$ ns and $\tau_2 = 17.5$ ns.

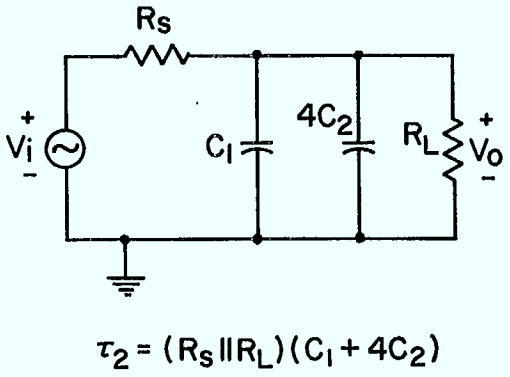

Fig. 7(b). Equivalent to (a) with the switch in position 1.

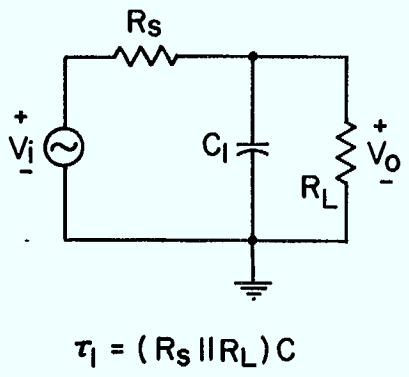

Fig. 7(c). Position 2 where r_d has been assumed equal to zero.

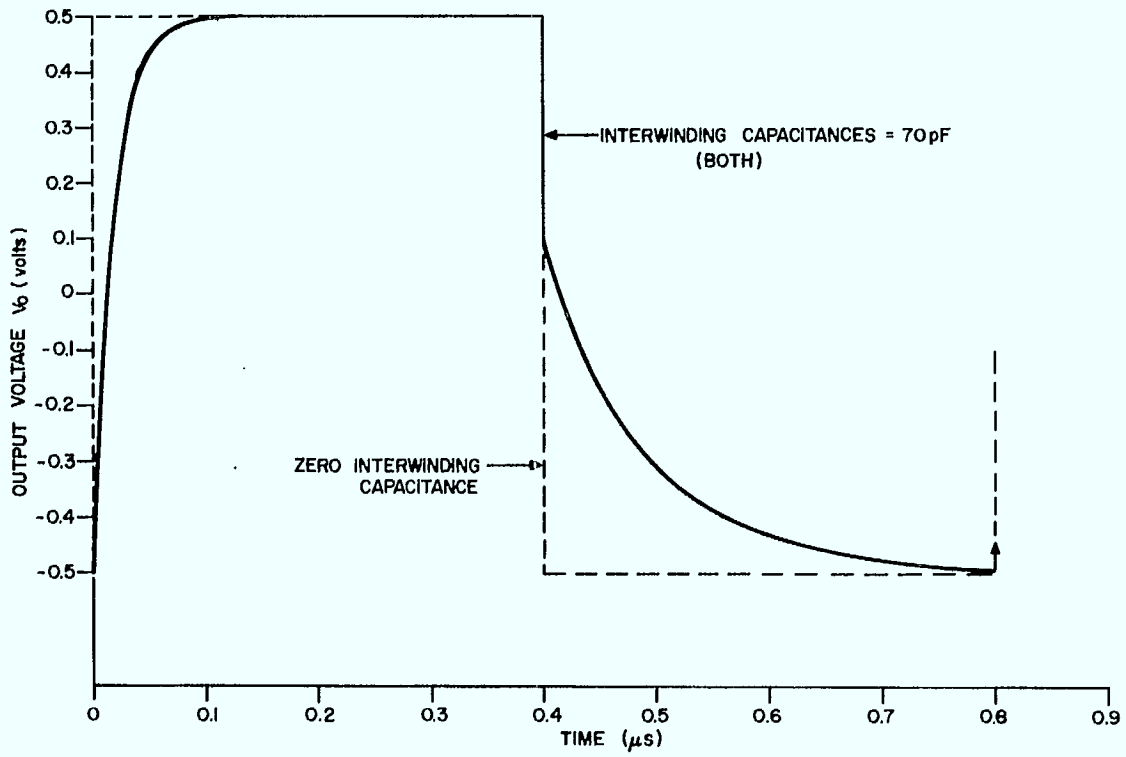

Fig. 8. Output voltage waveform of circuit in Fig. 7(a) for $C_1 = C_2 = 70$pF and for $C_1 = C_2 = 0$. The source voltage is assumed to be constant at 1V.

* These results were obtained using an ECAP transient analysis program in which the transformer in Figure 7 (a) was simulated by using a system of interdependent sources.

Also shown in Figure 8 is the output voltage for $C_1 = C_2 = 0$. The difference between these curves represents a power loss which, although dissipated in R_L and R_S, may be considered as caused by C_1 and C_2. For the waveforms shown in Figure 8, the loss is greater than 1 dB. To reduce this loss, transformer T1 was rewound in the configuration indicated in Figure 9 (b) using insulating material of low dielectric constant (teflon). The interwinding capacitances, C_1 and C_2 were reduced to approximately 7 pF each with resultant time constants of $\tau_1 \cong 9$ ns and $\tau_2 \cong 2$ ns.

The system shown in Figure 10 with the parameter values indicated was then constructed. This system, with the lowpass filter and series tuned circuit replaced by suitable source and load resistances, gave a conversion loss of 4.2 dB. It was decided to obtain measurements with 3, 4 and 5 pole Butterworth lowpass filtered inputs in order to assess the effects of various impedance characteristics on system performance. The lowpass filters used and their impedance and insertion loss frequency responses are indicated in Figures 11 to 14.

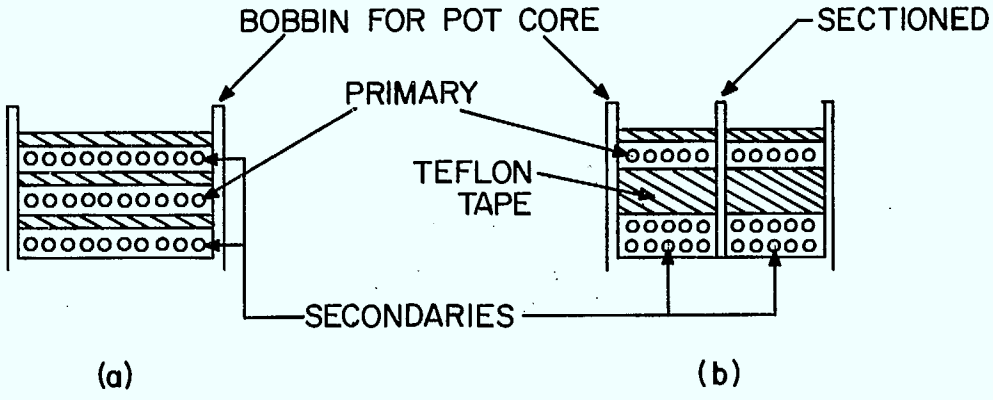

Fig. 9. Transformer T1 winding cross-section for (a) transformer as originally used (b) transformer as wound for low interwinding capacitance.

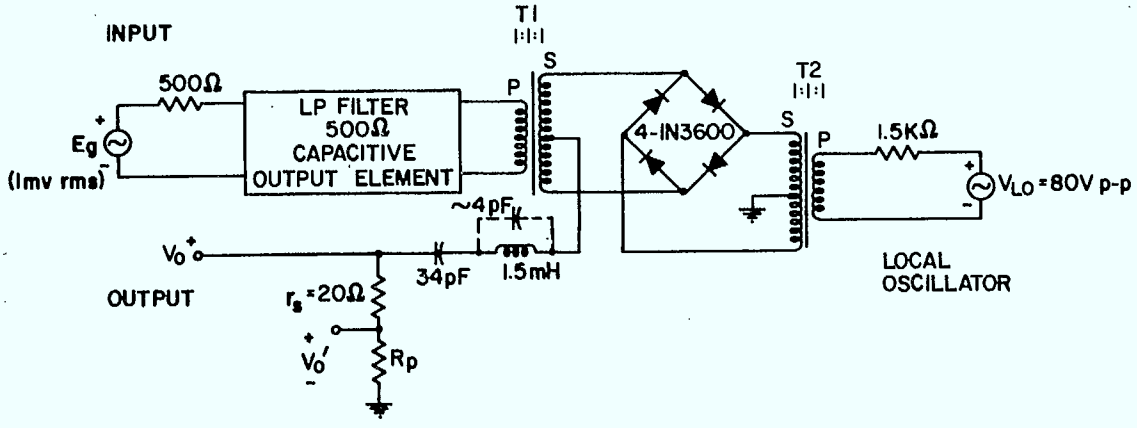

	T1	T2
PRIMARY INDUCTANCE Lp	2.25 mH	128 μH
INTERWINDING CAPACITANCE C_{iw}	10 pF	—
SHUNT INTERTURN CAPACITANCE C_s	62 pF	12 pF
LEAKAGE INDUCTANCE ℓ	14 μH	0.86 μH

Fig. 10. Low frequency, low conversion loss, wideband input mixer system.

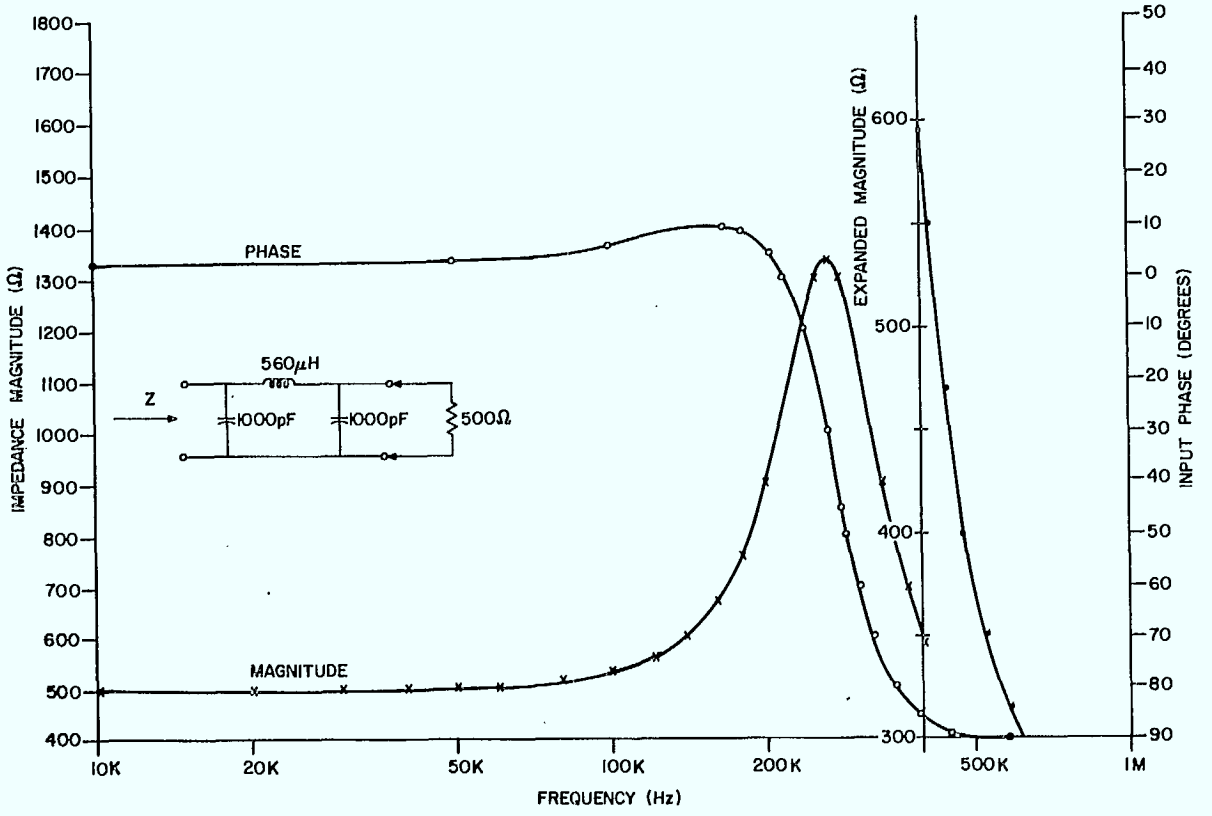

Fig. 11. Impedance response of 500Ω 3-pole Butterworth lowpass filter measured on a HP 4800A vector impedance meter.

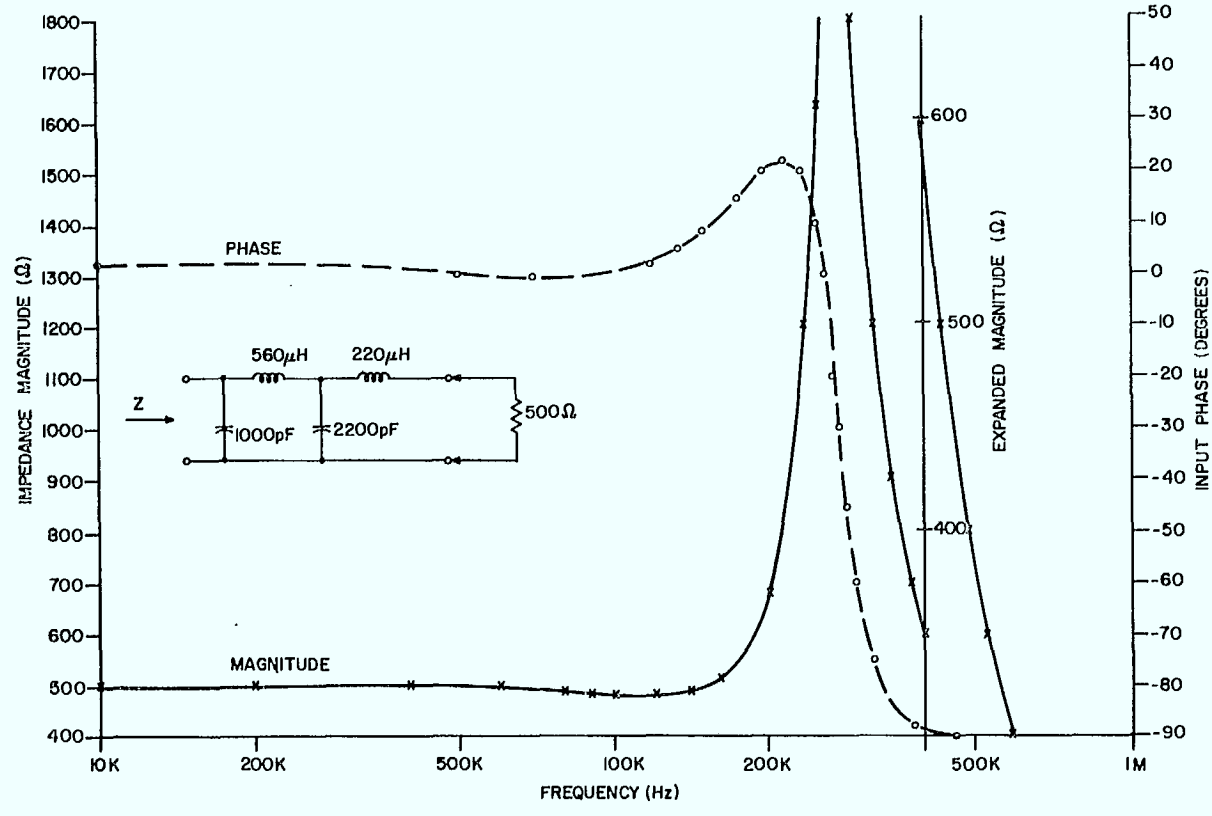

Fig. 12. Impedance response of 4-pole Butterworth lowpass filter as measured at the capacitive terminals on a HP 4800A vector impedance meter.

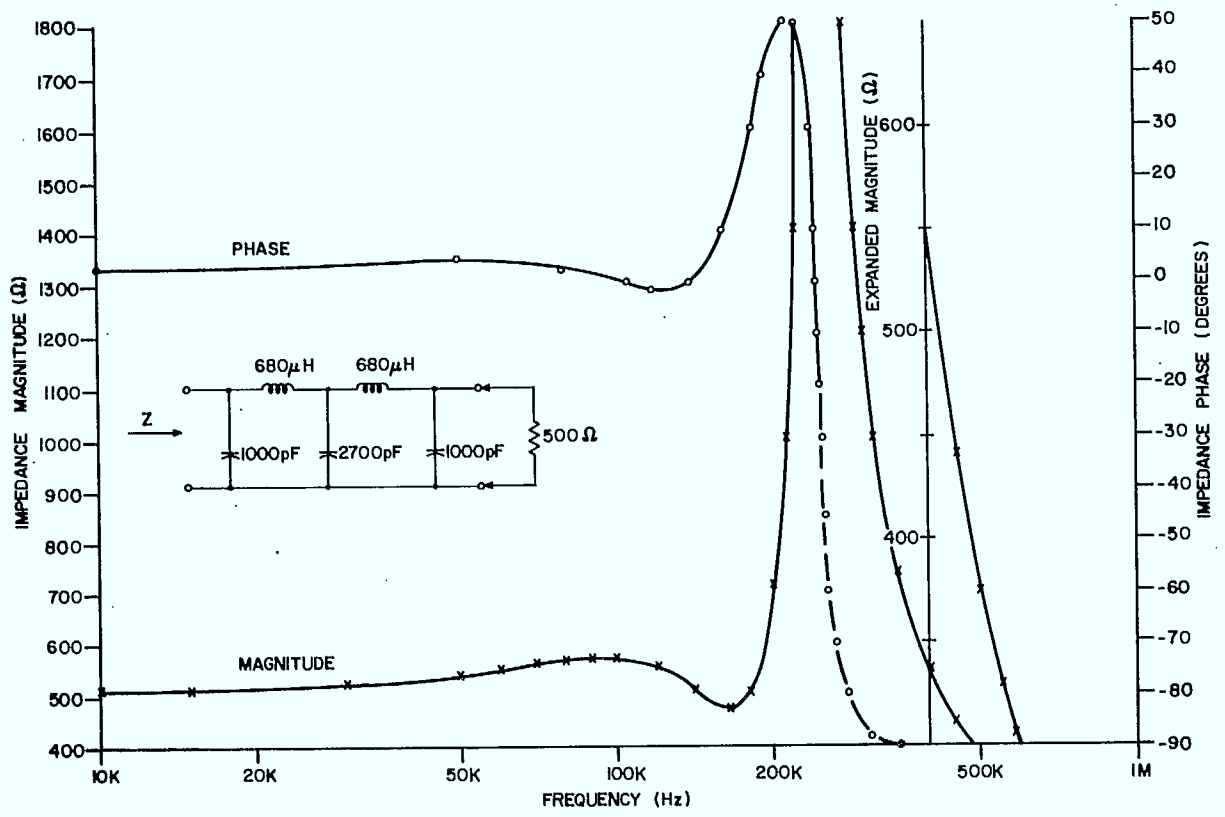

Fig. 13. Impedance response of 5-pole Butterworth lowpass filter measured on a HP 4800A vector impedance meter.

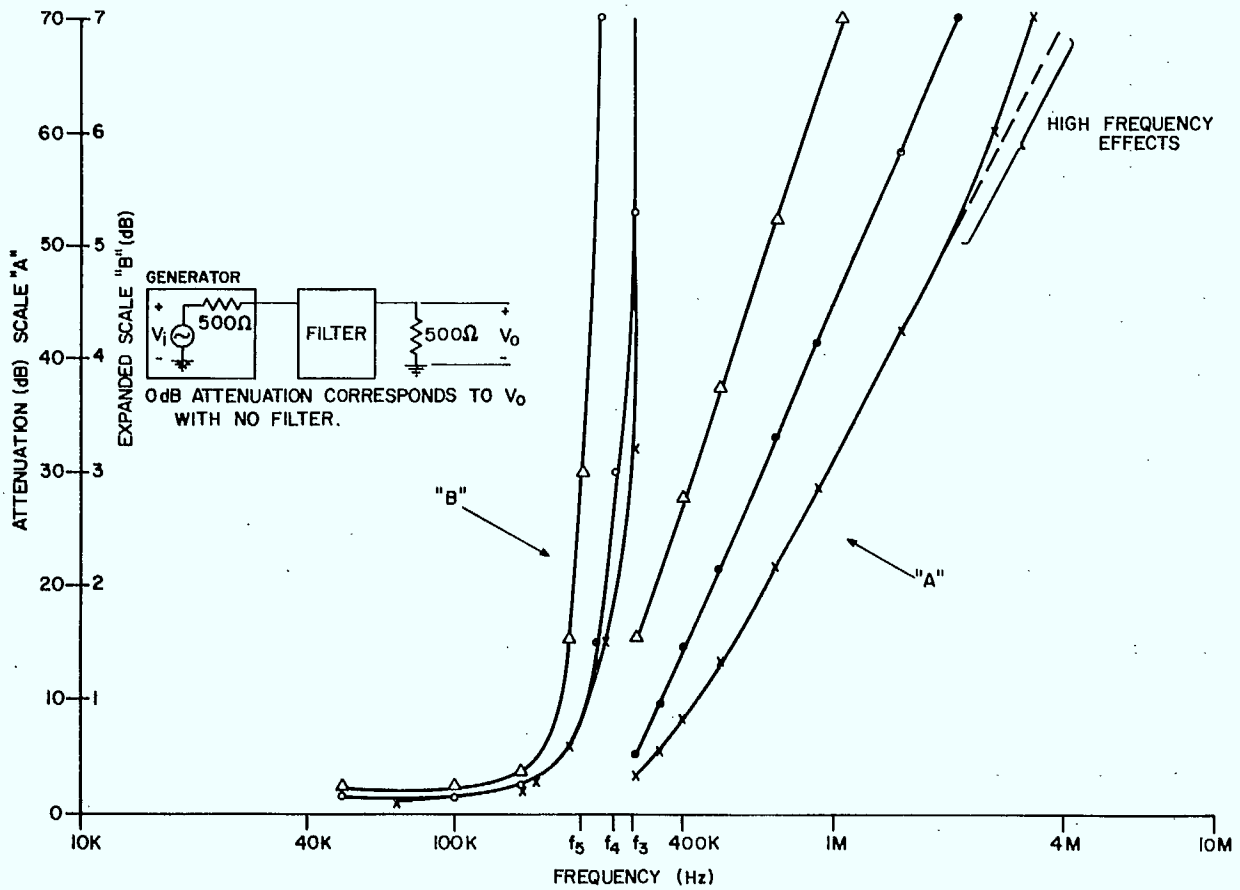

Fig. 14. Attenuation frequency responses of 3-, 4- and 5-pole Butterworth lowpass filters. The frequencies $f_3 = 217$ kHz, $f_4 = 270$ kHz and $f_5 = 296$ kHz correspond to the 3 dB corner frequencies of the 3-, 4- and 5-pole filters respectively.

For a 500 Ω source impedance, the theoretically optimum value of R_L should be $R_L = \frac{4}{\pi^2} \times 500 = 203\ \Omega$. However, it was decided to vary the load resistance from 100 Ω to 500 Ω to evaluate its effect on the mixer conversion loss. The resultant IF circuit Q could therefore drop to as low as 6 and climb to as high as 30. As in the narrowband case, the effective load resistance was again taken to be the sum of the external load resistance R_P and the series loss resistance r_s. The system used to measure the conversion loss is shown in Figure 15.

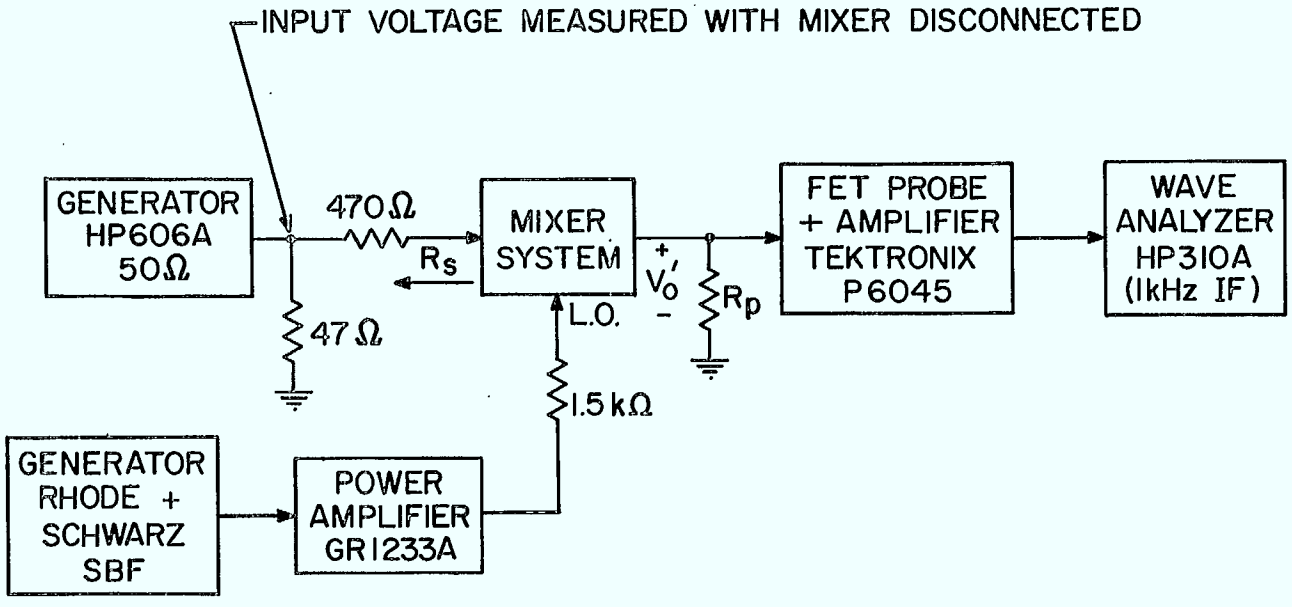

Fig. 15. Mixer conversion loss measurement system.

The dependence of conversion loss on load resistance for various selected frequencies is shown in Figures 16, 17 and 18 for the 3, 4 and 5 pole Butterworth lowpass filters, respectively. It is obvious from these curves that the optimum value of load resistance R_{Lopt} is in general substantially higher than the calculated value of $R_L = \frac{4}{\pi^2} R_S = 203\Omega$.

It may be shown that this effect is mainly a result of the variations in filter insertion loss caused by terminating the filter in an impedance other than its characteristic impedance. To illustrate this, curves indicating the variation in filter insertion loss with terminating impedance are included in Figures 16, 17 and 18 for the specific cases of signal frequencies equal to, first of all, 100 kHz and, secondly, approximately equal to the 3 dB frequencies of the filters.* It is obvious that these curves, when added to the theoretical (ideal) performance curves, will result in higher effective values of R_{Lopt}, in particular at the higher signal frequencies. At low signal frequencies, it may be seen that this effect will be less pronounced. However, at low signal frequencies, a secondary effect begins to appear and may be accounted for by the effect of X_{eq} as embodies in equation (4) and illustrated in Figure 6. For example, if X_{eq} is very small, then the optimum value of R_L is $R_{Lopt} = \frac{4}{\pi^2} R_S \cong 200\Omega$. However, if $X_{eq} = R_S$, then $R_{Lopt} = 0.55\ R_S \cong 275\Omega$ and if $X_{eq} = 2R_S$, then $R_{Lopt} = 0.9\ R_S \cong 450\Omega$. It may therefore be expected in practice to find R_{Lopt} for minimum conversion loss to be somewhat greater than $\frac{4}{\pi^2} R_S$. Furthermore, since X_{eq} increases (for the filters used) as the signal frequency is decreased, it may also be expected that this effect will appear mainly at the lower input frequencies. It should also be noted that as R_L is decreased, the higher ratio of diode ON resistance to load resistance may contribute further loss.

* These curves are theoretical and were obtained using computer-aided design techniques.

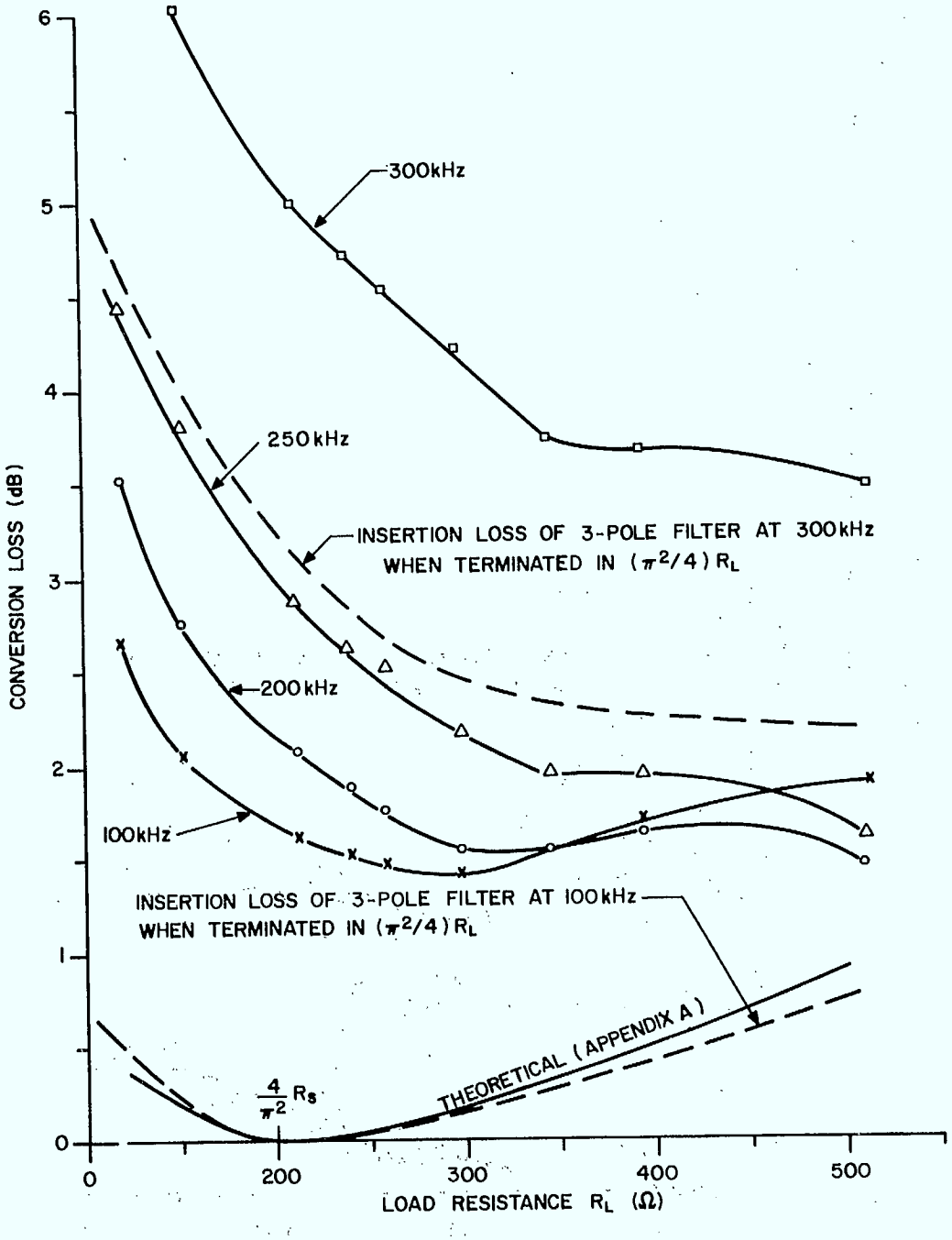

Fig. 16. Conversion loss variation with load resistance for the mixer with a 3-pole Butterworth lowpass filtered input (f_c = 296 kHz) as functions of the input signal frequency. The theoretical curve refers to the conversion loss with ideal terminations as indicated in Appendix A. The dashed lines refer to the insertion loss of the filter when terminated in a resistance $R = \frac{\pi^2}{4} R_L$ equal to the input resistance of the mixer when terminated in R_L.

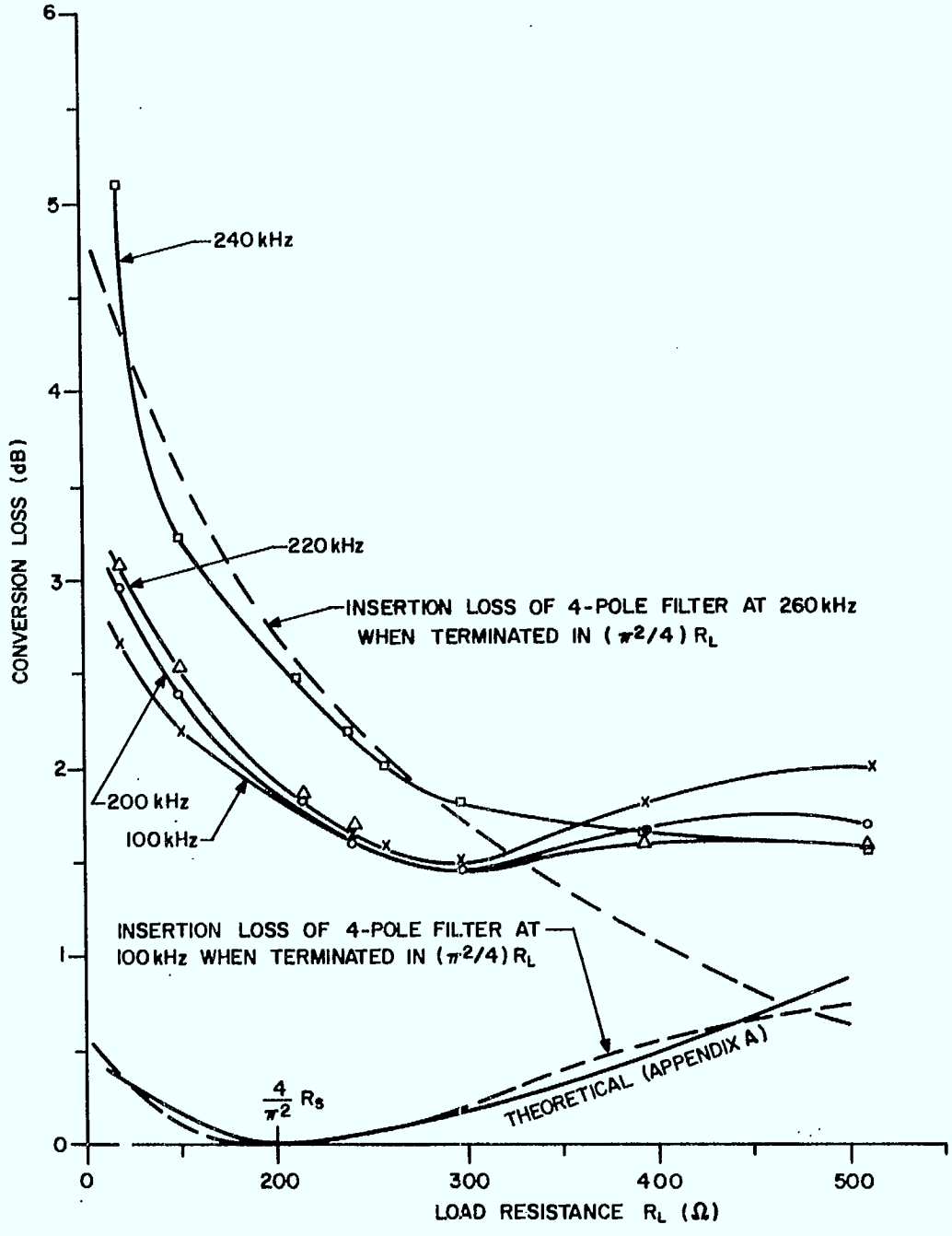

Fig. 17. Conversion loss variation with load resistance for a mixer with a 4-pole Butterworth lowpass filtered input (f_c = 270 kHz).

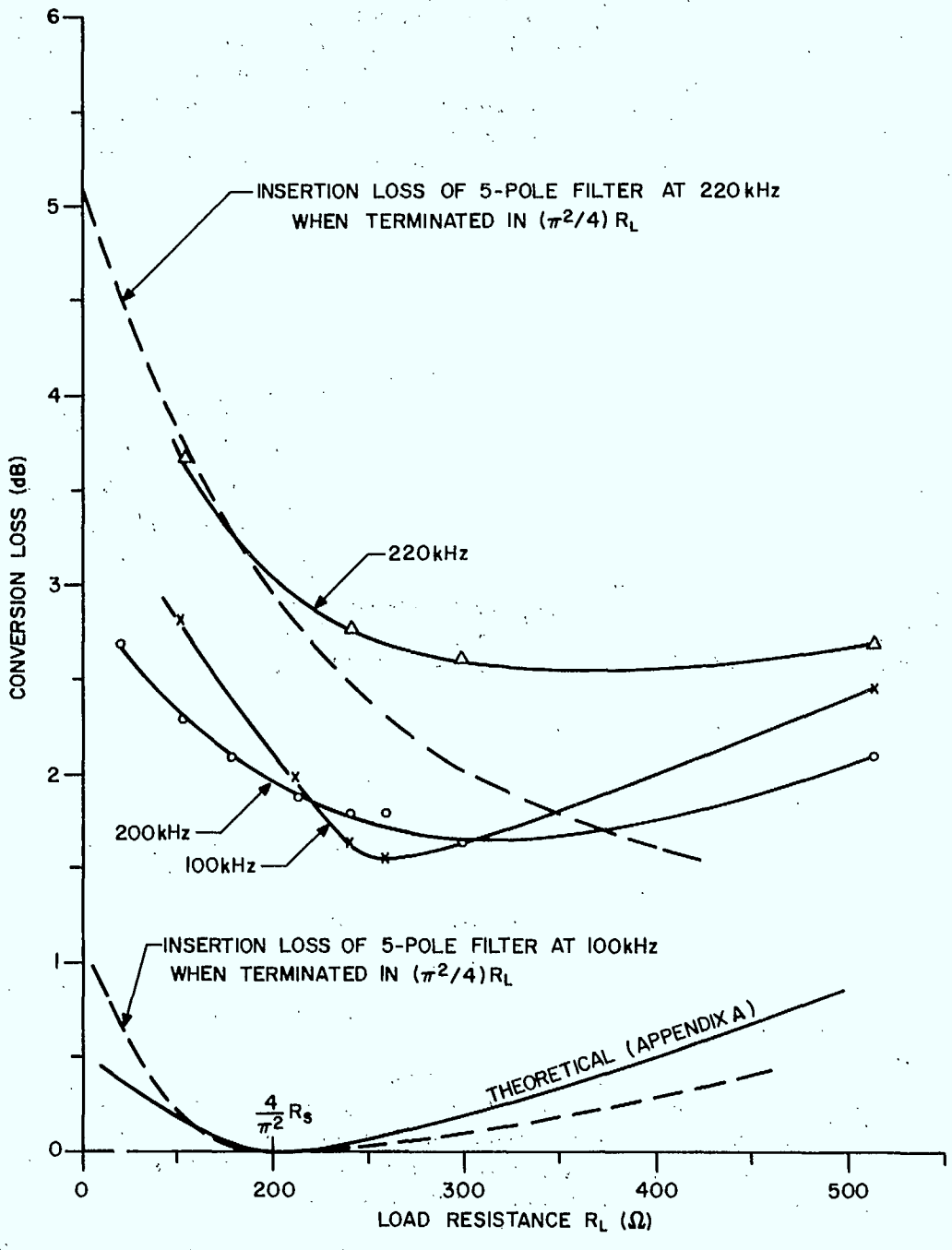

Fig. 18. Conversion loss variation with load resistance for a mixer with a 5-pole Butterworth lowpass filtered input (f_c = 217 kHz).

The conversion loss frequency responses for the mixer with its input terminated in each of the three lowpass filters are shown in Figure 19. The values of load resistances used in each case were selected using the curves of Figures 16, 17 and 18 and were, for the 3 pole lowpass filtered input case $R_L = 260\Omega$ and for the 4 and 5 pole cases $R_L = 300\Omega$. The 1.5 to 2.0 dB conversion losses in the system passbands constitute an improvement of 2.0 to 2.5 dB over that of the resistively terminated mixer. In all cases the increase in conversion loss with frequency may be seen to coincide very closely with the increase in the lowpass filter insertion loss as the cutoff frequency is approached. Also noticeable in Figure 19, in particular for the 4 and 5 pole cases, is a distinct fluctuation in conversion loss for input frequencies of about 100 kHz to 150 kHz. For these signal frequencies, the 3 p-q frequency components at the output of the circuit occur at 2.3 MHz to 2.4 MHz which, it was found, coincides with the self-resonant frequency of the inductor in the series tuned output circuit. This coincidence should result in a decrease in conversion loss at these frequencies. However, in the case of the 4 pole lowpass filtered input case, the conversion loss actually increased. The cause of this effect was not determined.

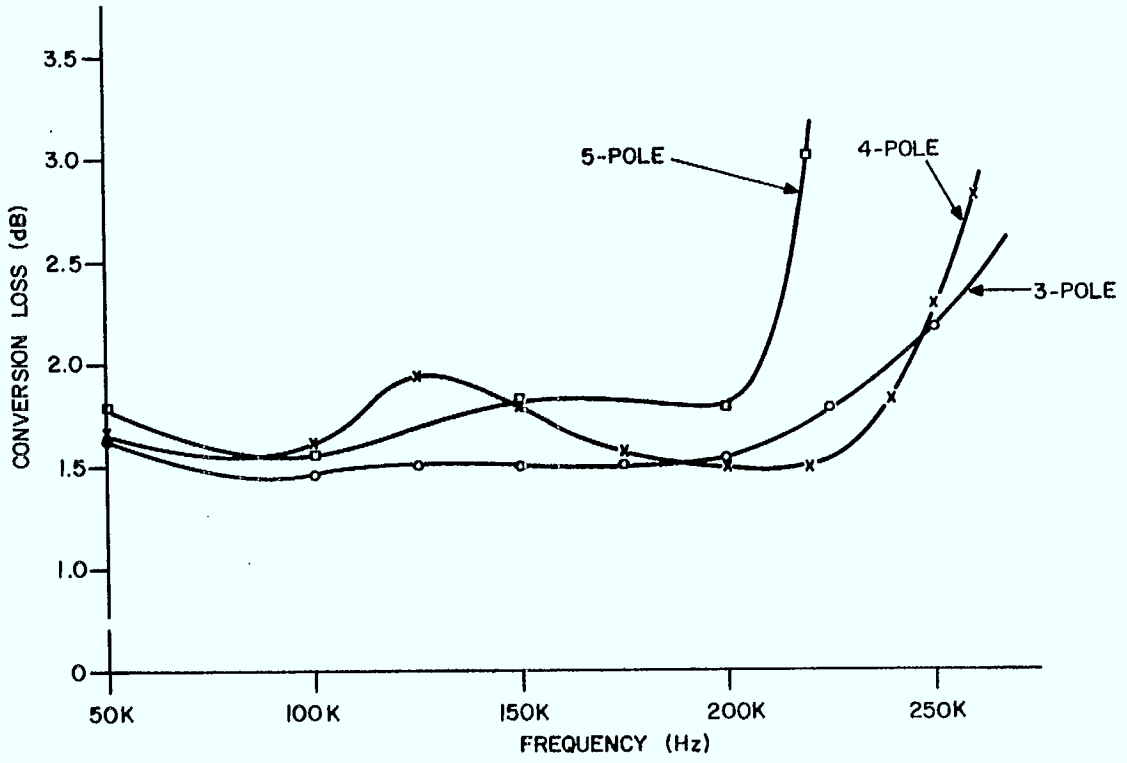

Fig. 19. Conversion loss of the mixer terminated at its input by 3-, 4- and 5-pole Butterworth lowpass filters. The load resistances were 260Ω, 300Ω and 300Ω, respectively.

In conclusion, a system is described which is capable of 1.5 to 3.0 dB conversion loss for a 50 kHz to 275 kHz signal frequency with an IF frequency of 700 kHz. Furthermore, the results indicate that an even wider band of operation might be obtained by increasing the lowpass filter bandwidths. These results verify the ability to obtain low conversion loss frequency translation for systems whose inputs are wideband by using diode ring modulators terminated in frequency selective impedances.

In the above results, the series loss resistance in the IF tuned circuit was included in the conversion loss calculation as part of the load, to conform more closely to the theoretical operation of the system. If this resistance is not taken into account, the conversion loss is downgraded by approximately 0.4 dB for the values of load resistances used in obtaining the system frequency responses. This results in a wideband (50 to 225 kHz) conversion loss of 1.9 to 2.4 dB, still a substantial improvement over the resistively terminated case.

3. HIGH FREQUENCY INVESTIGATION

3.1 CHOICE AND EVALUATION OF A SYSTEM CONFIGURATION

As mentioned in the introduction, this study was originally initiated to investigate the feasibility of incorporating a low conversion loss mixer system into the ISIS-B and the proposed ISIS-C sounder receivers. Having indicated the feasibility of designing low frequency wideband mixer systems capable of less than 4 dB conversion loss over an input frequency range of greater than 6 to 1, it remained to investigate the problems encountered in extending these results to include the high RF frequencies encountered in the sounder program (up to 20 MHz).

The first system to be considered had the configuration shown in Fig. 20(a). However, it was found that in order to obtain a sufficiently high Q in the tuned output stage, both a very low value of transformer primary inductance as well as a very high value of load resistance R_L would be required. Typically, the minimum practical value of transformer primary inductance is of the order of 1μH. For a nominal value of load resistance of $R_L = 500\Omega$, this value corresponds to a loaded Q at 20 MHz of approximately unity. To obtain a Q of 10, it would therefore be necessary to use an R_L of 500Ω. This value, as well as being of the same order of magnitude as typical values of transformer shunt resistance, by equation (12) requires a value of source resistance and

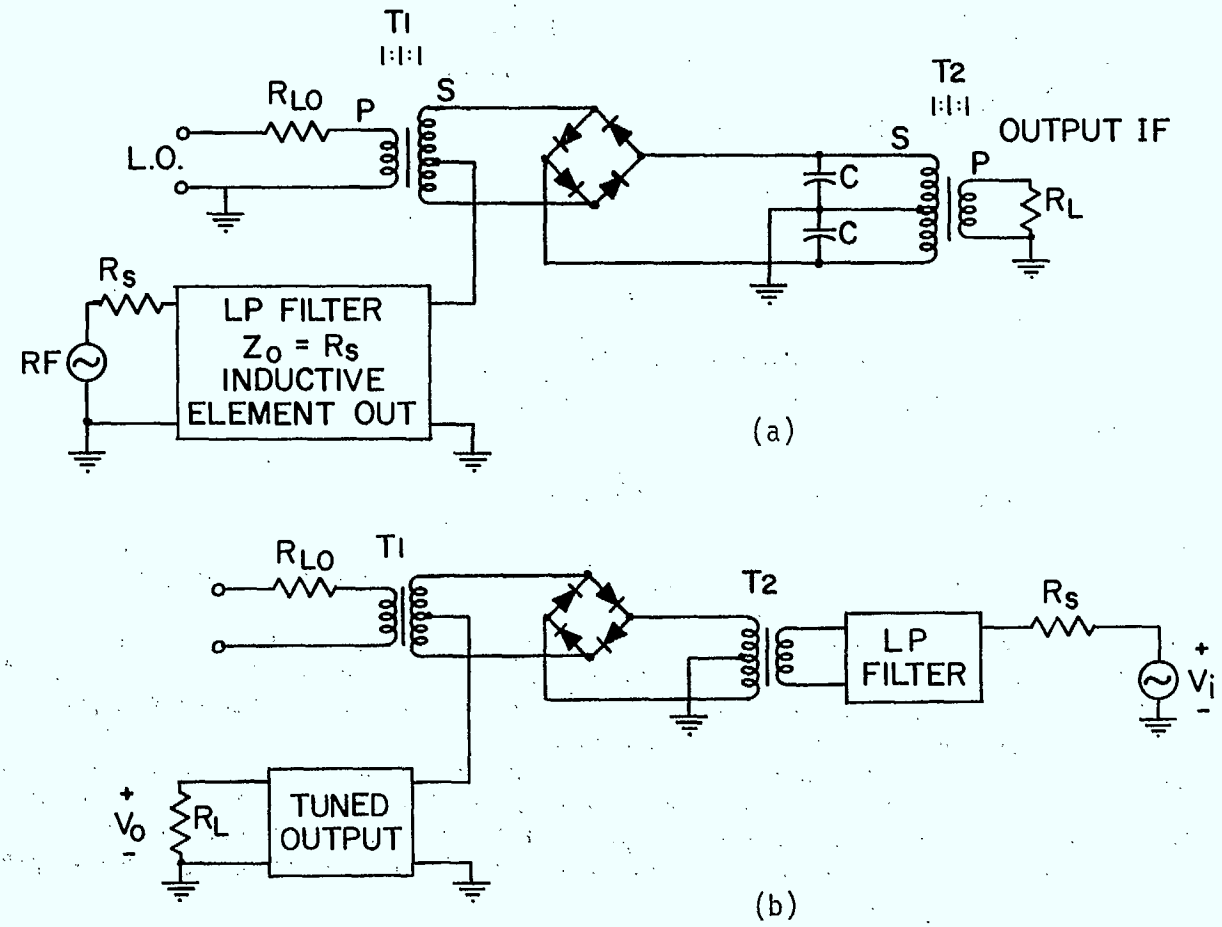

Fig. 20. Wideband input mixer configurations
(a) tuned transformer output
(b) wideband transformer input.

therefore lowpass filter characteristic resistance of $R_S \cong 2k\Omega$. Filters with characteristic impedances as high as this require 15 to 20 μH inductors which have, typically, self resonant frequencies of approximately 25 MHz for RF chokes and as low as 50 MHz for air core inductors. Obviously, such self resonances can severely alter the impedance response of the lowpass filter.

The dual of the system in Figure 20 (a), obtained by interchanging the input and output ports, is shown in Figure 20 (b). This system has the decided disadvantage that transformer T2 is required to transform a wide band of frequencies with a high degree of fidelity.

An alternative to the above two systems is shown in Figure 21. With this system, no transformers appear in the signal flow path except indirectly. Also, for the case where inductor L in the tuned output stage is the same as the primary inductance of T2 in Figure 20 (a), the output circuit Q is improved by a factor of four over that in Figure 20 (a). Therefore, a circuit with the configuration shown in Fig. 21 was built.

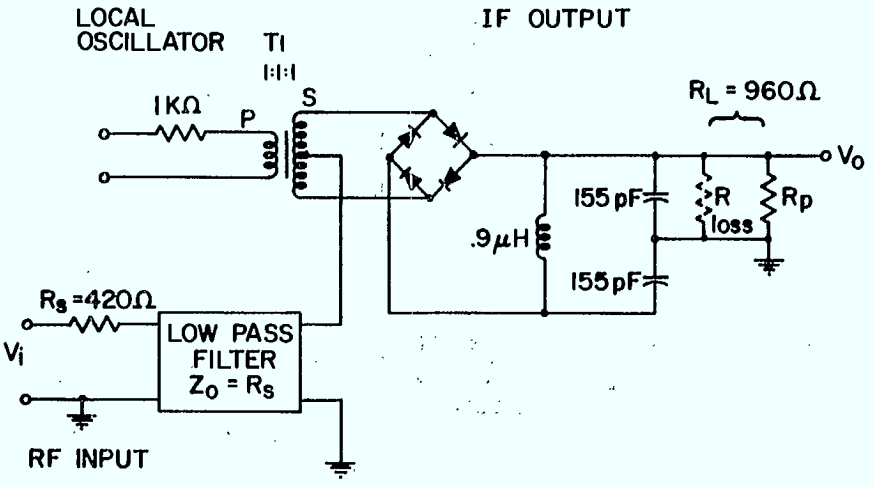

T1 L_p = 1.9μH = PRIMARY INDUCTANCE

C_{iw} = 2.2 pF = INTERWINDING CAPACITANCE

ℓ = .23μH

DIODES - IN4307 MATCHED DIODE QUAD.

Fig. 21. Wideband input mixer system with balanced-to-unbalanced matching network output.

Preliminary measurements made with an 8 MHz input frequency and without the input lowpass filtered indicated conversion losses of approximately 4.6 dB with a very strong dependence on LO level. Since the LO transformer being used had an interwinding capacitance of 10 pF, the transformer was redesigned specifically to give a low interwinding capacitance. With the new transformer (parameters as indicated in Figure 21) and with a 1N4307 high speed, high conductance, low capacitance, matched diode quad to replace the HPA 5082-1002 1002 diodes originally used, the minimum conversion loss decreased to 3.8 dB at 8 MHz. Since the conversion loss again exhibited a strong dependence on LO level, and since 3.8 dB is less than the predicted minimum conversion loss of 3.92 dB for this particular configuration, it was decided that further investigation was needed to determine the cause of these unusual effects.

Although the mixer did not appear to be performing as expected, it was nevertheless decided to investigate the frequency dependence of the mixer conversion loss and the effect of lowpass filtering the input signal. The lowpass filter used was a modified Butterworth 4 pole lowpass filter for which the impedance response and circuit diagram are shown in Figure 22. The modifications were necessary to accommodate and, by locating the resultant impedance peak near the 2p-q image frequency range, to make use of, the input inductor self-resonance. It was also decided to include the filter as an integral part of the mixer system since it was found that the capacitances of the BNC coaxial cable connectors greatly affected the impedance of the filters. The conversion loss variation with frequency for both the resistive input and for the lowpass filtered input case are shown in Figure 23. To obtain these results the LO level was adjusted to give the minimum conversion loss at each frequency. It is obvious from Figure 23 that, since the conversion loss for the resistive input case is already very low, the effect of the lowpass filter is, in general, a downgrading of the conversion loss performance. It was decided at this point to investigate further both the strong dependence of conversion loss on LO drive level and the cause of the low conversion losses obtained with the input resistively terminated.

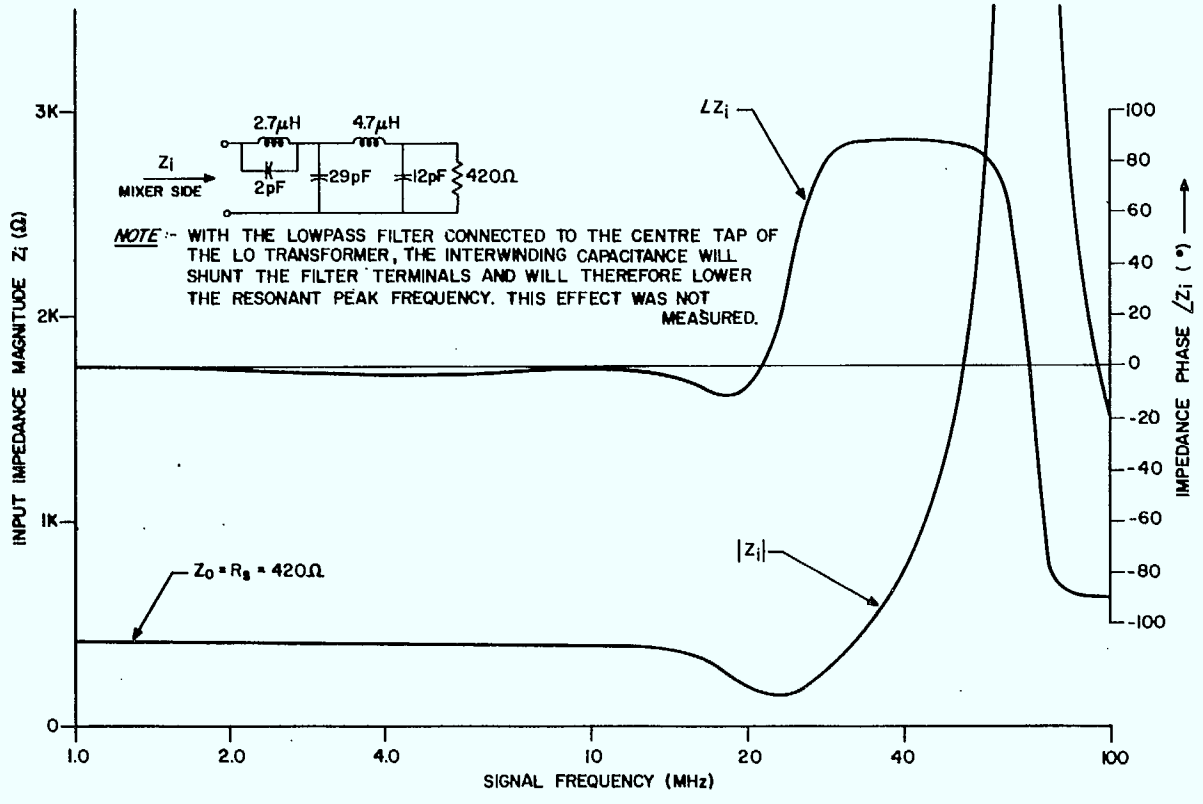

Fig. 22. Impedance response and circuit diagram of the modified 4-pole Butterworth lowpass filter.

3.2 INVESTIGATION OF LOW CONVERSION LOSS PHENOMENON FOR RESISTIVELY TERMINATED MIXER

To ensure that the unexpectedly low conversion loss of the mixer with resistive input termination was not a property peculiar to the 1N4307 diodes, the 1N4307 diode quad was replaced successively by 1N3600's, 1N916A's and, a Schottky barrier diode quad, the HPA2374. This latter was included to investigate the possibility that the anomalous behavious might be related to the phenomenon of charge storage as explained by Colin and Salzmann[12] and Gardiner and Howson[13]. In their analyses, it is indicated that if, as a result of charge storage, the time taken for the diodes to change state is equal to one-third of the switching period, then all terms of order 3n, n odd, may be eliminated from the mixer modulation function, with a corresponding reduction in conversion loss. The results for the various diodes are plotted in Figure 24 as functions of the

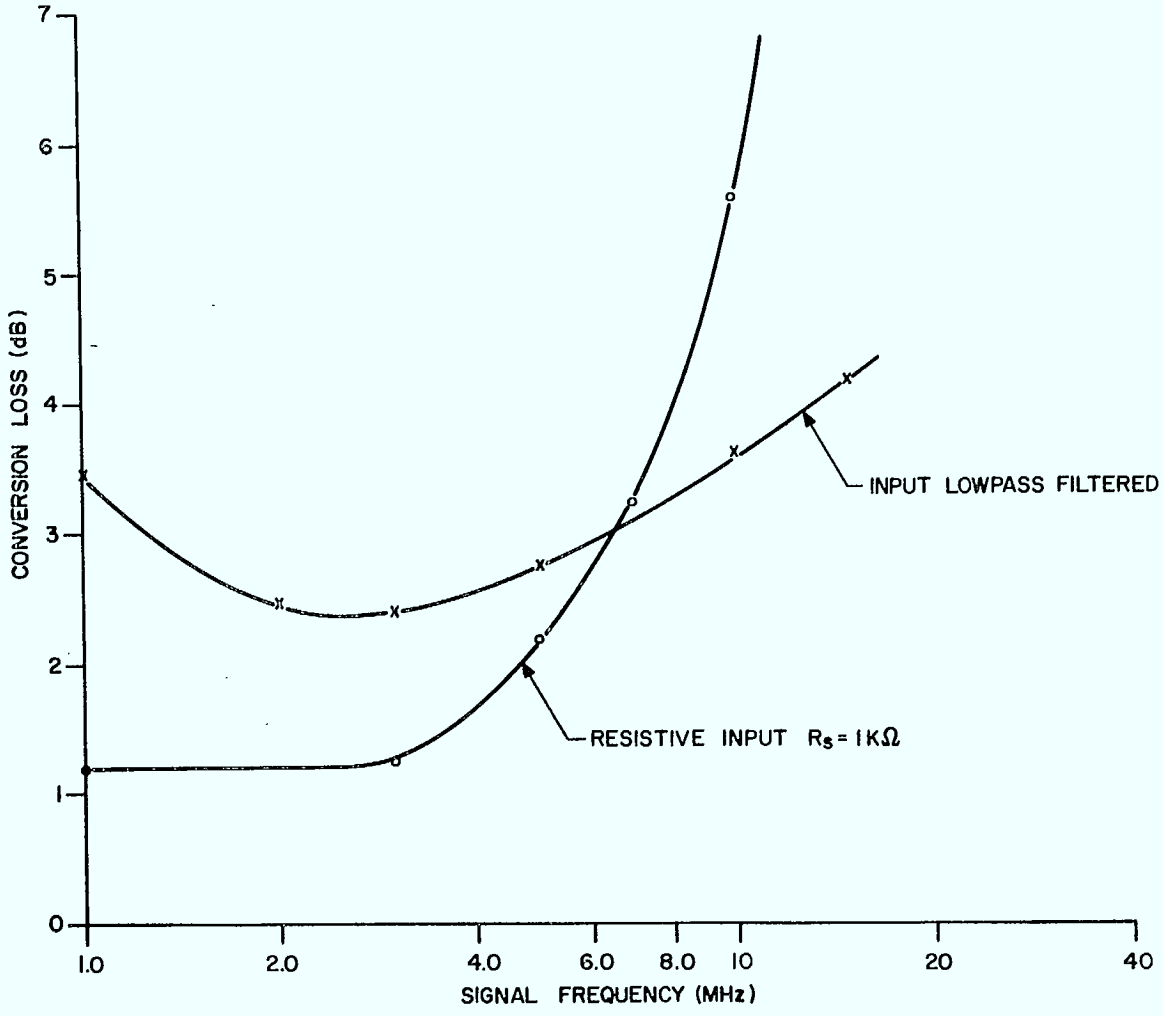

Fig. 23. Conversion loss frequency response of high frequency wideband diode ring mixer for both the resistive and lowpass filtered input cases.

peak LO current per diode and for a signal frequency of 5 MHz. The values of R_S and R_L used to obtain these results were adjusted to 1kΩ and 960Ω respectively where R_L is equal to R_P in parallel with the tuned circuit equivalent shunt loss resistance (see Fig. 21). The RF signal open circuit level was adjusted to approximately 9 mV rms. The LO current was measured in the secondary of T1 using a Rhode and Schwarz USVH selective microvoltmeter equipped with a Tektronix P6020 current probe. The input and output voltages were measured using the same microvoltmeter equipped with a Tektronix P6046 differential high impedance probe.

It is obvious from the results in Figure 24 that for each of the diodes used, the mixer conversion loss exhibits to varying degrees a marked dependence on LO drive level. However, in the case of the HPA 2374 Schottky barrier diodes, this anomalous barrier is not as pronounced. This would tend to support the theory that the unusual behaviour was an effect of charge storage since Schottky diodes exhibit essentially no charge storage. However, without the effects of charge storage, the minimum conversion loss with the HPA 2374 should be 3.92 dB and not 3.6 dB as obtained. In addition, the effect of charge storage would be, at best, to reduce the mixer conversion loss to a minimum of 3.6 dB for the configuration shown[12] and not 1.75 dB and 2.2 dB as obtained for the 1N3600's and the 1N4307's respectively.

To investigate the function of the tuned output circuit in the anomalous performance of the mixer conversion loss, the tuned output circuit was replaced by a center tapped autotransformer of inductance $L_P = 29\mu H$ and the 1N4307 diodes were replaced. Although the self resonant frequency of the autotransformer occurred at 22 MHz and was chosen as the output frequency, with the source resistance adjusted to 420Ω and the effective load resistance (again incorporating the autotransformer losses) adjusted to 430Ω , the output was essentially wideband with a measured 3 dB frequency range of 8 MHz to 75 MHz. The conversion loss variation with LO drive level was again measured and is included in Figure 24. It is obvious from these results that the elimination of the tuned output resulted in a very noticeable decrease in the conversion loss dependence on LO drive level and a corresponding increase in conversion loss from 2.2 dB to 4.6 dB. This behaviour would suggest the possibility that the tuned output circuit might be acting as a form of idler circuit.

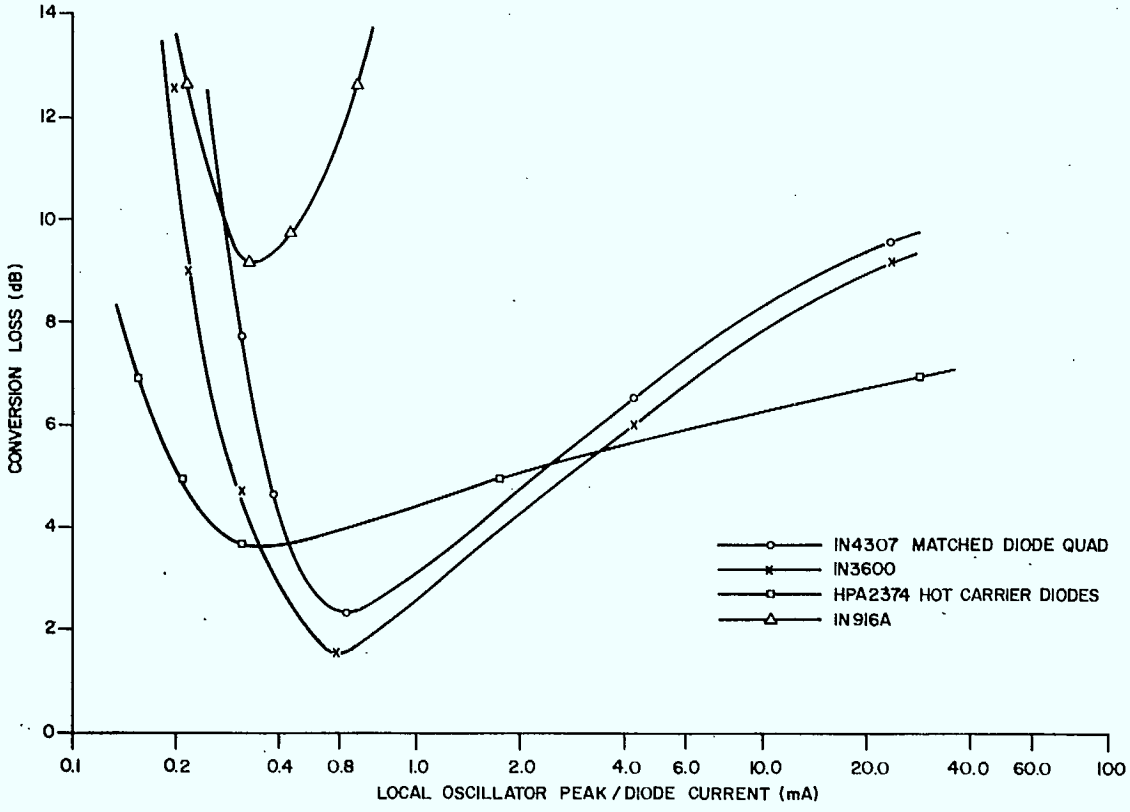

Fig. 24. Conversion loss of diode ring mixers using various diodes as functions of the local oscillator drive current and for a signal frequency of 5 MHz.

Before proceeding further with the investigation, it was decided to remove as much as possible all frequency dependence from the output circuit by replacing the output circuit with a center tapped resistor of value $2R = 930\Omega$, as shown in Figure 25 (a). With the output measured differentially across this output resistor, this system may be shown to be equivalent, with respect to the signal path, to a system with a center tapped output transformer. This is illustrated in Figure 25 (a) where the diode ring is represented by a system of switches. Note in Figure 25 (a) $v_0^2 = (v_1 + v_2)^2 = v_1^2 + v_2^2 + 2v_1v_2 = v_1^2 + v_2^2$ since at all times one of v_1 or v_2 is zero. Therefore, the output power is given by

$$P_0 = v_1^2/R + v_2^2/R = \frac{v_1^2 + v_2^2}{R}$$

$$= \frac{v_0^2}{R}$$

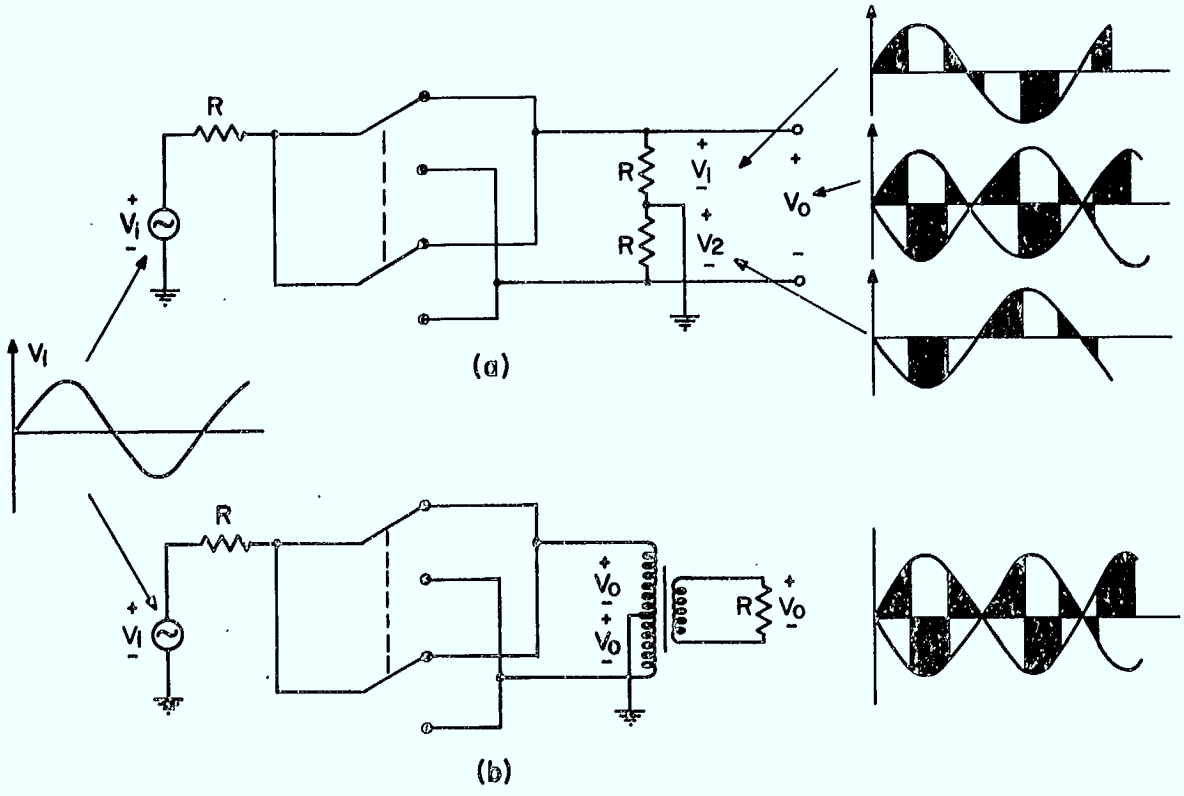

Fig. 25. An illustration of the equivalence between
(a) the center-tapped resistor output and
(b) the center-tapped autotransformer output.

The output power in Figure 25 (b) is $P_0 = v_0^2/R$ and, since it is obvious that v_0 is the same in this case as in Figure 25 (a), the output powers for the two systems are identical. Note also that this equivalence is maintained as long as v_1 and v_2 in Figure 25 (a) do not overlap in time. The conversion loss performance of the system with the center tapped resistor was measured and is shown in Figure 26. The close similarity between these results and those for the autotransformer output case may be considered to constitute proof of the equivalence of the two systems in Figure 25 (a) and (b).

Due to the strong dependence of mixer conversion loss on LO drive level, and due to the substantial decrease in conversion loss with the addition of the tuned output circuit, it was postulated that the anomalous behaviour might be caused by varactor effects. This postulate is based on the supposition that the power series describing the variation of the varactor junction capacitance with the voltage contains a substantial linear (zero order) term. In this case it is theoretically possible to draw power from the LO and dissipate it in the load at the IF output frequency. However, only if the coefficient of the zero order term is sufficiently large will the power contributed by the LO be substantial and will the reduction in mixer conversion loss be significant. It may be expected that a larger capacitance variation with voltage will occur for a varactor diode rather than a diffused or Schottky diode. For this reason, it was decided to replace the mixer diodes with four Varian VAT 73ET 12.0 to 15.9 pF abrupt junction varactor diodes. The resultant conversion loss variation with LO drive level is included in Figure 26 and the variation with signal frequency is shown in Figure 27. It is obvious from these results that some IF output power is being derived from the LO since the mixer system actually displays a conversion gain of as high as 6.3 dB. Due to lack of time, a more extensive investigation of these effects was not performed. Points to be investigated could include the effects of:

(a) tuning one or the other or both of the input and output ports,

(b) using varactor diodes of different zero bias junction capacitances,

(c) using hyper-abrupt junction varactor diodes (whose junction capacitance varies approximately as V_D^{-2} rather than $V_D^{-1/2}$ as it does for the abrupt junction diode),

(d) changing the operating frequency range from HF to VHF or MF.

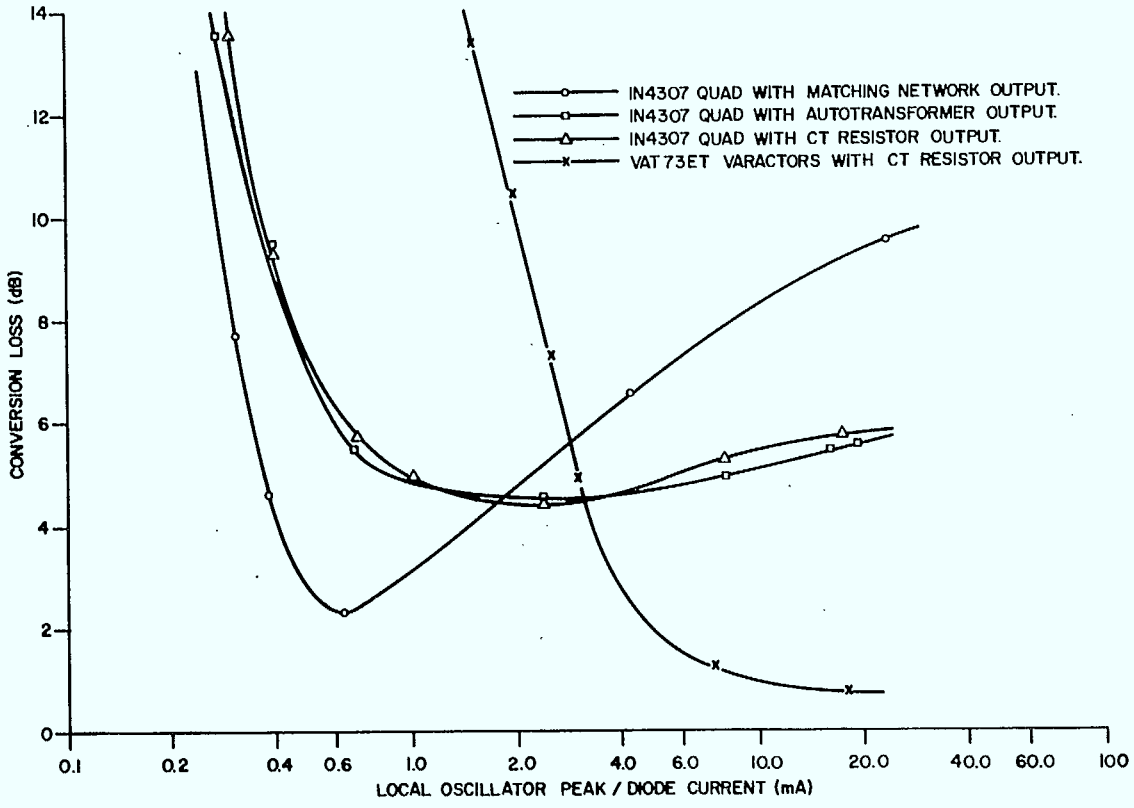

Fig. 26. Conversion loss of diode ring mixers using various output circuit configurations as functions of the LO current and using a 1N4307 matched diode quad at a 5 MHz signal frequency. Included is the conversion loss of a diode ring mixer using VAT73ET varactor diodes.

4. A RECEIVER SYSTEM WITH MIXER INPUT*

4.1 INTRODUCTION

A typical superheterodyne receiver front end is shown in Figure 28(a). In general such systems are evaluated with respect to two basic performance criteria: intermodulation (IM) performance and sensitivity or noise figure. The noise figure of the system in Figure 26(a) is, in general, determined primarily by the noise figure of the RF amplifier since the effect of the noise figure of the mixer and tuned IF amplifier on the system noise figure is reduced by a factor equal to the RF amplifier gain. Likewise, the IM performance of the receivers is, especially for wideband RF cases, largely determined by the IM performance of the RF amplifier.

---

* The system to be described is based on a concept introduced by R.J. Bonnycastle in his report *A Study of Low-Noise Wide Dynamic Range Radio Frequency Front End Amplifiers*[4]. This same report may be consulted for general results concerning IM performance and noise figures.

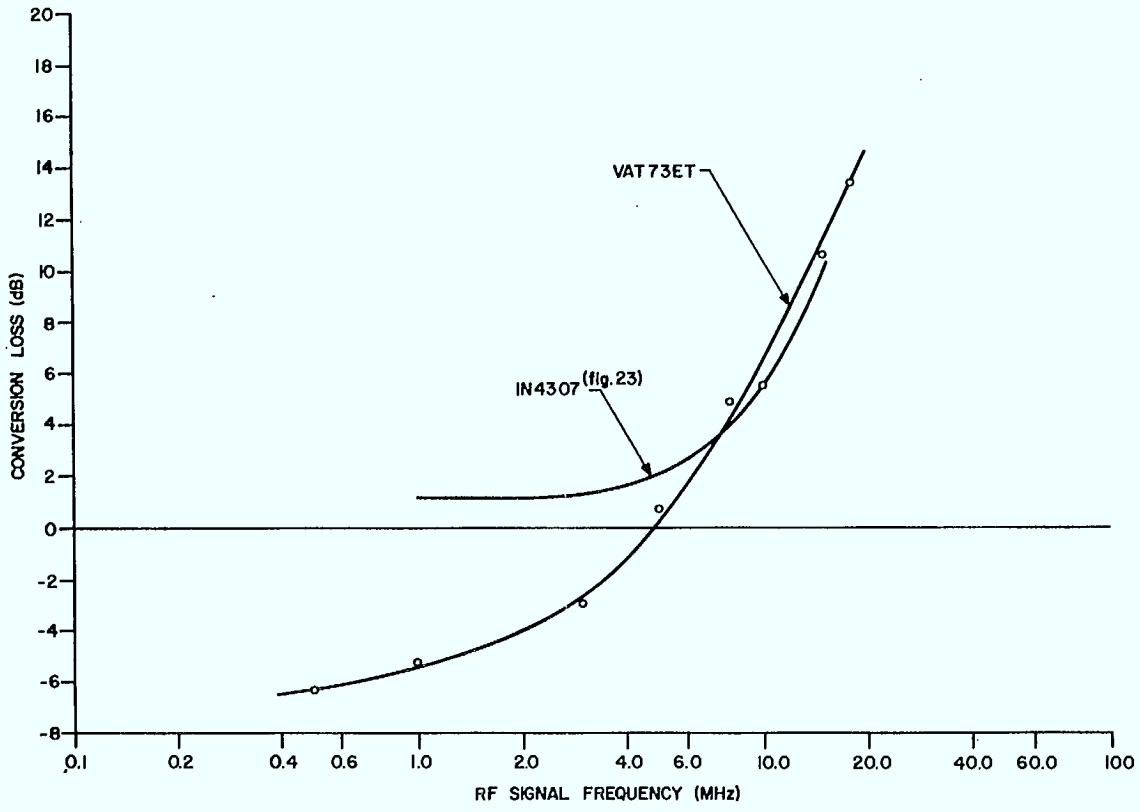

Fig. 27. Conversion loss variation with signal frequency for a 1N4307 matched diode quad and for four VAT73ET varactor diodes. The LO level is adjusted in each case to give minimum conversion loss.

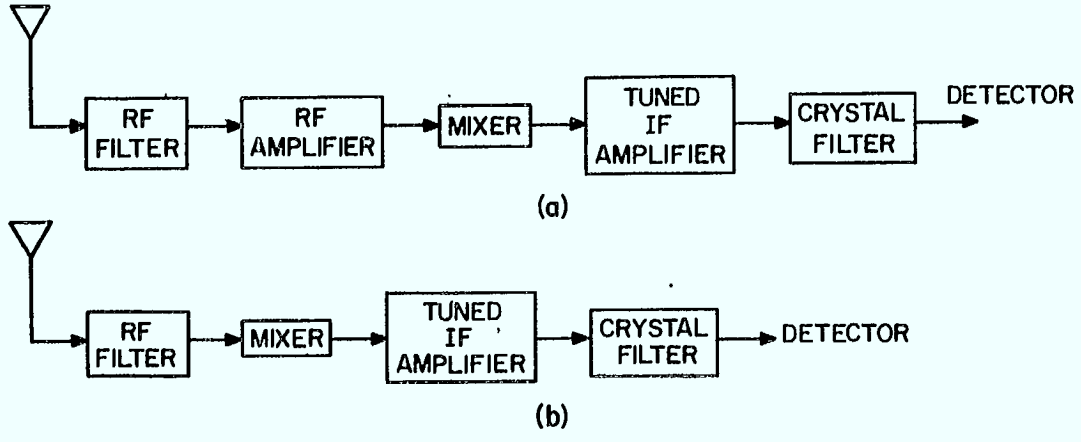

Fig. 28. (a) A typical superheterodyne receiver front end (b) an alternative.

An alternative form of superheterodyne receiver front end in which the RF amplifier is eliminated altogether is shown in Figure 28 (b). Besides eliminating the IM distortion which normally occurs in the RF amplifier, the removal of RF amplification results in lower signal levels at the inputs of the mixer and tuned IF amplifier. Such a reduction in signal levels results in a reduction in the IM contributions of the mixer and IF amplifier[14] with a corresponding further improvement in the overall system IM performance. However, since the elimination of the RF amplifier also results in the system noise figure now being determined by the IF amplifier and mixer stages, it is therefore necessary for these stages to have as low noise figures as possible.

4.2 ANALYSIS OF A RECEIVER SYSTEM WITH MIXER INPUT

A system designed to meet the above specifications is shown in Figure 29. It should be noted that this system is designed on the basis of noise figure and not power loss since, using lossless components and an infinite input impedance FET amplifier IF stage, the power loss of this system will be infinite.

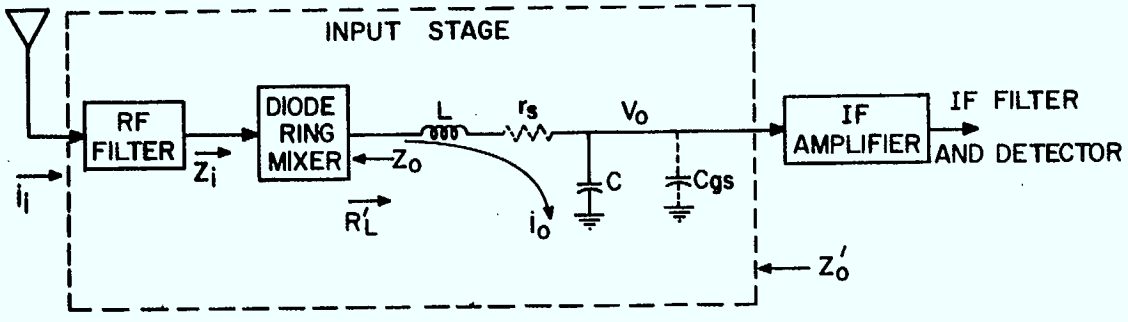

Fig. 29. A receiver front end without RF amplification

The noise figure of this system is very difficult to evaluate although tentatively it may be estimated as follows. Using Friis's equation for the noise figure of cascaded stages[15], the system noise figure is given by

$$NF_T = NF_{IS} + \frac{NF_{IF} - 1}{G_m}$$

where NF_T = noise figure ratio of system
NF_{IS} = noise figure ratio of input stage
NF_{IF} = noise figure ratio of IF stage
G_m = available gain of input stage.

For reasons which will later become apparent, the series tuned L-net has been included in the input stage and is considered to assimilate the gate-to-source capacitance of the FET amplifier stage. For the moment, consider the input filter to be a parallel tuned circuit tuned to the signal frequency and consider also that the antenna may be replaced by a current source of value i_g in parallel with a resistance R_g. From Appendix A, the current gain of a ring mixer terminated in this fashion is given by

$$\frac{i_g}{i_L} = \frac{2}{\pi} + \frac{\pi}{2}\frac{R_L'}{R_g} \qquad \ldots\ldots (18)$$

where R_L' is the equivalent load resistance as seen by the mixer. Also from Appendix A, the mixer output impedance at the IF frequency is $Z_0 = \frac{4}{\pi^2} R_g$. Therefore, if the input stage is terminated in $Z_0' = Q^2(\frac{4}{\pi^2} R_g)$, where Q is the loaded Q of the series tuned circuit equal to $(2\pi f_{IF} L_S)/(4R_g/\pi^2)$, then the value of R_L' to be used in equation (18) is $R_L' = \frac{4}{\pi^2} R_g$. The maximum available gain G_m of the input stage is therefore given by

$$G_m \triangleq \frac{P_{o\ available}}{P_{i\ available}} = \frac{R_L' i_L^2}{R_g i_g^2/4} = \frac{(4R_g/\pi^2)(\pi i_g/4)^2}{R_g i_g^2/4} = 1$$

with the result that the system noise figure is reduced to $NF_T = NF_{IS} + NF_{IF} - 1$.

Furthermore, if it is assumed that the input stage noise contribution occurring as a result of component losses and diode dynamic resistances is negligible with respect to that from the source and load impedances, the system noise figure N_T is then equal to NF_{IF}. Also, by a suitable choice of impedance levels and field-effect transistor amplifier configuration, NF_{IF} may be made less than 1 dB. It is therefore theoretically possible using this system to obtain a receiver noise figure as good as and possibly better than even the best of super-heterodyne receivers which use RF amplifiers.

Unfortunately, the above analysis has many shortcomings. For one, the analysis is not readily extendible to the case where the RF filter is a lowpass filter. However (as shown in Section 1.2.2) for a suitable lowpass filter , the operation of such a system is quite similar to that with a parallel tuned input. The results when using a lowpass filter may therefore be expected to be somewhat similar to those developed above.

Another serious shortcoming of the above analysis is the assumption that the source impedance is totally resistive. Since the source in many cases will be an antenna having a large reactive component, and since this system is particularly dependent on terminating impedances, the system noise figure may be much worse than the analysis suggests. Unfortunately, an analysis of such a case is difficult to perform.

A further shortcoming of the analysis performed above is the assumption that the noise contributions occurring from the component and diode losses are negligible—an assumption which may not be valid when the mixer is selectively terminated. In particular, for low conversion loss (high G_m) operation, the impedance of the RF filter at the image and higher order unwanted frequency components must be very small. However, this causes the noise current occurring at these frequencies and resulting from the series mixer and L-network losses to be large with a correspondingly large noise contribution at the output. A further noise contribution comes from the LO and the RF sources as a result of direct feedthrough to the IF since, although the mixer is theoretically balanced to both the RF and LO ports, practical systems will always have some degree of unbalance and therefore feedthrough.

Although, as indicated, the noise figure analysis as presented has many shortcomings, the results indicate the possibility of obtaining a very low noise figure receiver front end. It was therefore decided to build and test such a system.

4.3 AN EXPERIMENTAL LOW NOISE FIGURE RECEIVER

To evaluate the performance of the above receiver configuration, the system shown in Figure 30 was built. The mixer used in this system is the equivalent of that used and described in Section 2.2 except that the external load resistance R_P used there has been eliminated. Also, the IF frequency has been changed to 500 kHz. The effective loaded Q of the tuned IF circuit is

$$Q = \frac{2\pi(500\ kHz)\ (1.5\ mH)}{(4/\pi^2)\ (500\Omega)} = 22.$$

The noise figure of the L-network followed by the FET amplifier was measured to be approximately 1 dB when operated from a 500Ω source.*

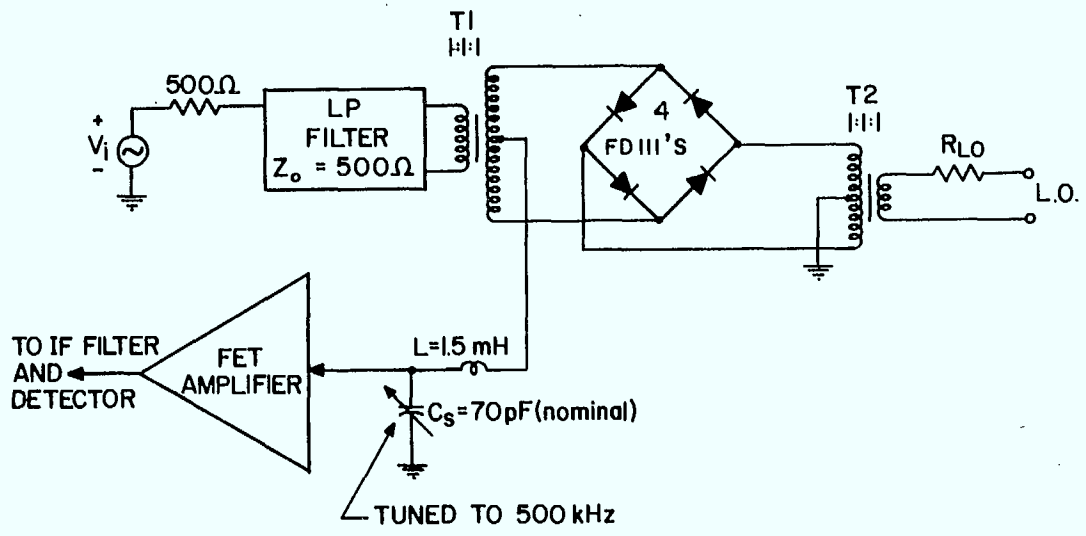

Fig. 30. Practical realization of system in Fig. 29. For the transformer specifications, see Fig. 10.

With no input filter and using FD111 diodes, the noise figure of this system was found to be 3 dB measured using the test arrangement shown in Figure 31 and for a local oscillator frequency of 700 kHz. With no input filtering, the noise generator is able to introduce noise at both the signal frequency and its image. Therefore, when the image is filtered out, the 3 dB noise figure obtained above should result in a new system noise figure of 4.76†. With the input signal shunt parallel tuned at 200 kHz, the noise figure was measured to be 5 dB. However, when the input was lowpass filtered by the 4-pole Butterworth lowpass filter shown in Figure 32, and connected with the generator at the inductive filter terminals, the noise figure (at 700 kHz LO frequency) rose to 6 dB. With the filter reversed, the noise figure increased further to 10 dB.

The FD111 diodes were then replaced by 1N3600's and a new transformer T1 wound (for low interwinding capacitance as described in Section 2.2. The unfiltered input noise figure then decreased to approximately 2.0, 2.0 and 3.0 dB at 75,225, and 525 kHz signal frequency, respectively. With the input lowpass filtered, the noise figure variation with frequency was as shown in Figure 33 for both the inductive input case and the capacitive input case.

---

* In operation, the source resistance for this network is $\frac{4}{\pi^2} \times 500\Omega = 203\Omega$. However, the difference in noise figure should not be substantial since the FET amplifier is, in both cases, effectively operating from a high impedance (mixer output impedance transformed by the L-network Q).

† This assumes that the change in the noise figure of the IF stage which occurs as a result of the impedance change caused by the introduction of a lowpass filter at the input does not substantially affect the noise figure of the system. If this assumption is true, then $NF_{Filtered} = 1 + NF_{Unfiltered}$ where the noise figures are those measured using the test arrangement shown.

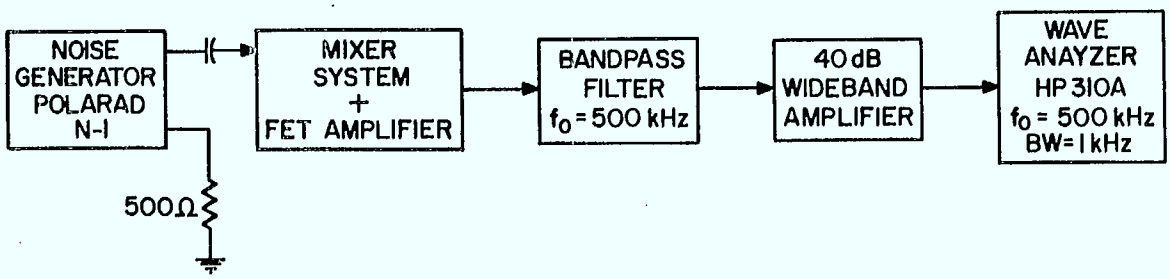

Fig. 31. Noise figure measurement system.

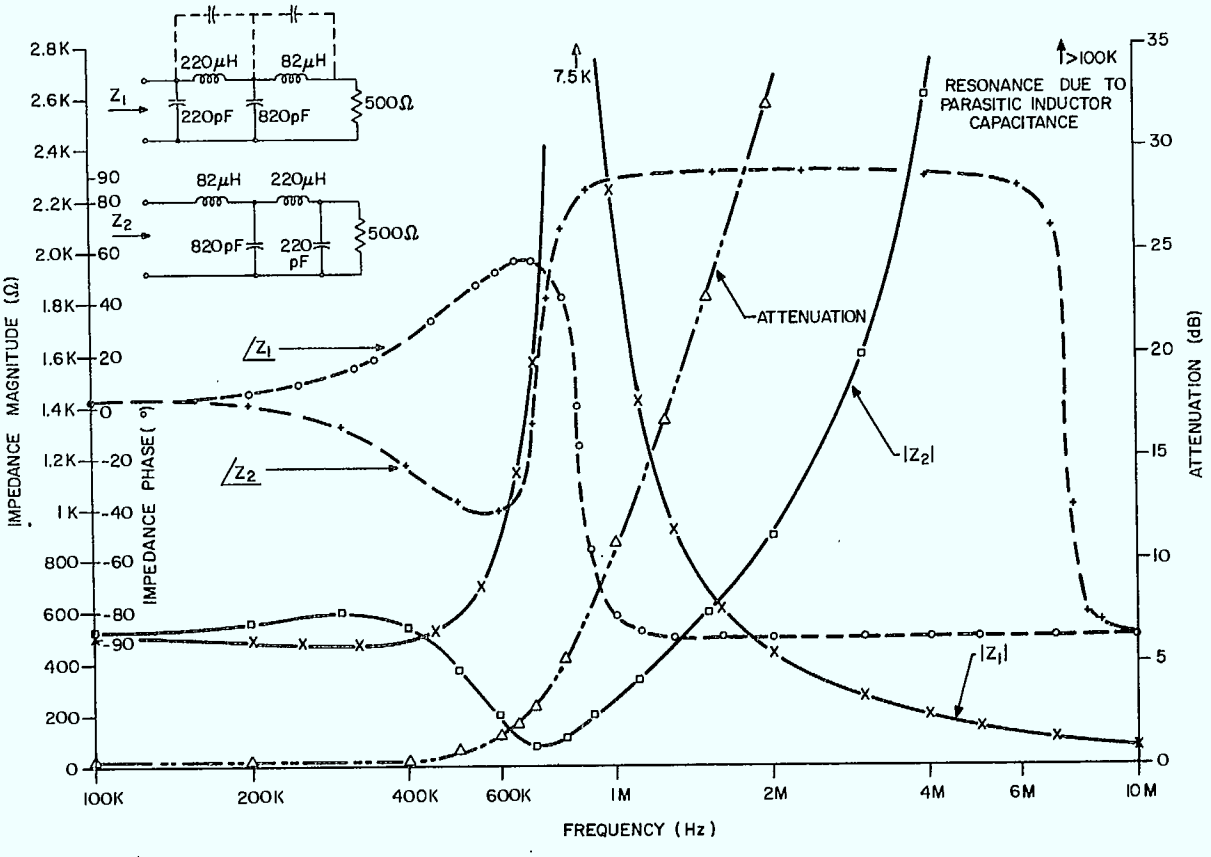

Fig. 32. Circuit diagram and impedance and attenuation response of the 700 kHz, 500Ω Butterworth lowpass filter.

The causes of the fluctuations in noise figure with frequency were not conclusively determined. However, some correlation was observed between the frequencies at which the fluctuations occurred and the impedance fluctuations of the lowpass filter and the series tuned output circuit. In particular, the large fluctuation which occurs at approximately 270 kHz (RF) corresponds quite closely to the coincidence of the 3p-q output sideband with the self resonant frequency of the 1.5 mH inductor (1.9 MHz). Also, some interaction between the lowpass filter and the series tuned circuit may be expected and such interaction could affect the noise figure variation with frequency. No definite conclusions could be drawn concerning the effects of the output impedance of the lowpass filter being capacitive or inductive since at the image frequency (2p-q), both filters presented

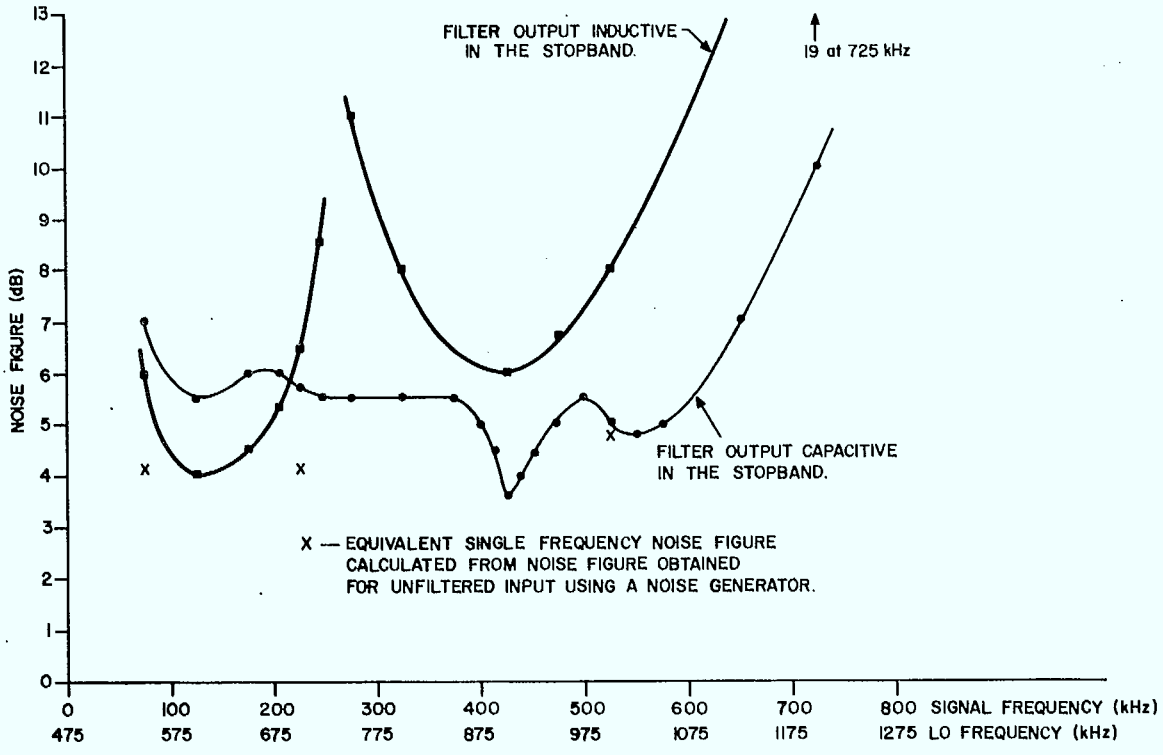

Fig. 33. Noise figure of mixer system with lowpass filtered input. The actual value of IF frequency used was 475 kHz (fixed by IF filter center frequency.

approximately the same impedance magnitude although the impedance phases were of the correct sign and magnitude. In general, the only conclusion to be drawn is that a wideband RF (100 kHz to 500 kHz), low noise figure (4 to 6 dB) system can be realized using this configuration. Further improvement may possibly be realized by investigating the effects of various alterations such as changing the lowpass filters, using other diodes and the effect of parallel rather than series tuning the output.

5. REFERENCES

1. Caruthers, R.S. *Copper Oxide Modulators in Carrier Telephone Systems.* Bell System Technical Journal, Vol 18, p. 315 - 337, 1939.

2. Tucker, D.G. *Rectifier Modulators with Frequency-Selective Terminations.* Proc. IEE, Vol. 96, Part III, p. 422 - 428, 1949.

3. Tucker, D.G. *Two Notes on the Performance of Rectifier Modulators, Part 1: The Input Impedance of Rectifier Modulators with Frequency-Selective Terminations.* Proc. IEE, Vol. 99, Part III, p. 400 - 402.

4. Gensel, Joachim. *Das Verhalten von Modulatorschaltungen bei Komplexen, Insbesondere Selektiven Abschlüssen.* Frequency, Vol. 11, No. 5, p. 153 - 159 and No. 6, p. 175 - 185, 1957.

5. Howson, D.P., and D.G. Tucker. *Rectifier Modulators with Frequency-Selective Terminations with Particular Reference to the Effect of Even-Order Modulation Products.* Proc. IEE, Vol. 107, Part B, p. 261 - 272, 1960. See also discussion IBID p. 283.

6. Tucker, D.G. *The Input Impedance of Rectifier Modulators.* Proc. IEE, Vol. 197, Part B, p. 273 - 281, 1960.

7. Salzmann, J. *Le Modulator en Anneau a Filtres Intégrés.* Cables et Transmission, Vol. 15, No. 2, p. 148 - 159 and No. 3. p. 186 - 189, 1961.

8. Kurth, Carl. *Analysis of Diode Modulators Having Frequency-Selective Terminations Using Computers.* Electrical Communication, Vol. 39, p. 369 - 378, 1964.

9. Lewis, H.D., and F.I. Palmer. *A High Performance High Frequency Receiver.* Presented at the IEEE Canadian Communications Symposium, Montreal, November, 1968.

10. Tucker, D.G. *Zero-Loss Second-Order Ring Modulator.* Electronics Letters, Vol. 1, No. 9, p. 245 - 246, 1965.

11. Tucker, D.G. *Second-Order Ring Modulator.* Proc. IEE, Vol. 113, No. 9, p. 1457 - 1462, 1966.

12. Colin, J.E., and J. Salzmann. *De Diverses Considerations sur les Modulateurs en Anneau, Premiere Partie: Interet et Realizations d'une Fonction de Commutation a Trois Etats dans les Modulateurs en Anneau.* Cables et Transmission, Vol. 22, No. 1, p..19 - 24, 1968.

13. Gardiner, J.G. and D.P. Howson. *Influence of Minority Carrier Storage on Performance of Semiconductor Diode Modulators.* Proc. IEE, Vol. 111, No. 8, p. 1393, 1964.

14. Bonnycastle, R.J. *A Study of Low-Noise Wide Dynamic Range Radio Frequency Front End Amplifiers.* CRC Report in preparation.

15. Friis, H.T. *Noise Figure of Radio Receivers.* Proc. IRE, Vol. 32, p. 419 - 422, July 1944.

APPENDIX A

Performance of Ring Modulators for Various Input and Output Terminations *

The performance of ring modulators for various input and output terminating conditions is tabulated in Table 1. The technique by which these results may be obtained will be illustrated by deriving the results for case 2 in Table 1.

TABLE 1

Case	Modulator Terminations				Modulator Input Impedance	Conversion Losses		
	Output Circuit		Output Circuit			Voltage	Current	Power
	Signal	Others	IF	Others				
1	R_g	R_g	R_L	0	$\dfrac{\frac{4}{\pi^2}}{\frac{1}{R_L}+\left(1+\frac{4}{\pi^2}\right)\left(\frac{1}{R_g}\right)}$	$\frac{\pi}{2}\left(1+\frac{R_g}{R_L}\right)$	$\frac{\pi}{2}\left(1+\frac{R_L}{R_p}\right)$	$\frac{\pi^2}{16}\left(\frac{R_g}{R_L}+2+\frac{R_L}{R_g}\right)$
2	R_g	∞	R_L	0	$\frac{4}{\pi^2}R_L$	$\frac{2}{\pi}+\frac{\pi}{2}\frac{R_g}{R_L}$	$\frac{\pi}{2}+\frac{2}{\pi}\frac{R_L}{R_g}$	$\frac{\pi^2}{16}\frac{R_g}{R_L}+\frac{1}{2}+\frac{1}{\pi^2}\frac{R_L}{R_g}$
3	Rg	R_g	R_L	∞	$\frac{\pi^2}{4}R_L+\left(\frac{\pi^2}{4}-1\right)R_g$	$\frac{\pi}{2}\left(1+\frac{R_g}{R_L}\right)$	$\frac{\pi}{2}\left(1+\frac{R_L}{R_g}\right)$	$\frac{\pi^2}{16}\left(\frac{R_g}{R_L}+2+\frac{R_L}{R_g}\right)$
4	R_g	0	R_L	∞	$\frac{\pi^2}{4}R_L$	$\frac{\pi}{2}+\frac{2}{\pi}\frac{R_g}{R_L}$	$\frac{2}{\pi}+\frac{\pi}{2}\frac{R_L}{R_g}$	$\frac{1}{\pi^2}\left(\frac{R_g}{R_L}+2+\frac{R_L}{R_g}\right)$
5	R_g	Rg	R_L	R_L	R_L	$\frac{\pi}{2}\left(1+\frac{R_g}{R_L}\right)$	$\frac{\pi}{2}\left(1+\frac{R_L}{R_g}\right)$	$\frac{\pi^2}{16}\left(\frac{R_g}{R_L}+2+\frac{R_L}{R_g}\right)$

* The results and analysis presented here are based on investigations performed by Caruthers[1], Tucker[2,6] and Tucker and Howson[5].

From Figure 1 (Section 2.1.1) it may be seen that case 2 corresponds to the input current being filtered to q while the output voltage is filtered to (p-q). Therefore, since the output voltage v_{34} is sinusoidal, it may be written $v_{34} = V\cos(p-q)t$. This voltage corresponds to an input voltage $v_{12} = y(t)v_{34}$ which, by equation (1), Section 2.1.1 has a component at frequency q which is equal to $(2/\pi)V\cos qt$. The input current i_{12} is also tuned and may therefore be written

$$i_{12} = \left(\frac{E}{R_g} - \frac{2}{\pi}V\right)\cos qt. \qquad \ldots\ldots (19)$$

This current, in passing through the mixer produced a current i_{34} given by $i_{34} = y(t)i_{12}$. Substituting for y(t) gives

$$i_{34} = \frac{2}{\pi}\frac{E}{R_g}[\cos(p-q)t + \cos(p+q)t - \frac{1}{3}\ldots] - \frac{4}{\pi^2}\frac{V}{R_g}[\cos(p-q)t + \cos(p+q)t - \frac{1}{3}\ldots]. \qquad \ldots\ldots (20)$$

Therefore,

$$\frac{V}{R_L}\cos(p-q)t = \cos(p-q)t\left[\frac{2}{\pi}\frac{E}{R_g} - \frac{4}{\pi^2}\frac{V}{R_g}\right] \qquad \ldots\ldots (21)$$

which by suitable manipulations yields the voltage conversion loss

$$\frac{E}{V} = \frac{\pi}{2}\frac{R_g}{R_L} + \frac{2}{\pi}. \qquad \ldots\ldots (22)$$

The current conversion loss is given by

$$\frac{J_g}{I_L} = \frac{E/R_g}{V/R_L} = \frac{2}{\pi}\frac{R_L}{R_g} + \frac{\pi}{2}. \qquad \ldots\ldots (23)$$

The power conversion loss is given by

$$L = \frac{\text{maximum power available from the source}}{\text{power delivered to the load}}$$

$$= \frac{E^2/4R_g}{V^2/R_L} = \frac{1}{4}\frac{R_L}{R_g}\left(\frac{E}{V}\right)$$

$$= \frac{\pi^2}{16}\frac{R_g}{R_L} + \frac{1}{2} + \frac{1}{\pi^2}\frac{R_L}{R_g}. \qquad \ldots\ldots (24)$$

The input resistance is given by

$$R_i = \frac{v_{12}(q)}{i_{12}(q)} = \frac{\frac{2}{\pi}V}{\frac{E}{R_g} - \frac{2}{\pi}\frac{V}{R_g}} = \frac{R_g}{\frac{\pi}{2}\frac{E}{V} - 1}$$

$$= \frac{R_g}{\frac{\pi^2}{4}\frac{R_g}{R_L}} = \frac{4}{\pi^2} R_L . \qquad \ldots\ldots (25)$$

The results for cases 1, 3, 4, 5 may be obtained similarly although cases 1 and 3 are somewhat more tedious due to the necessity of multiplying a Fourier series (such as (20)) by y(t).

Figure A-1 illustrates the variation in power conversion loss for the various cases as functions of the generator-to-load impedance ratio.

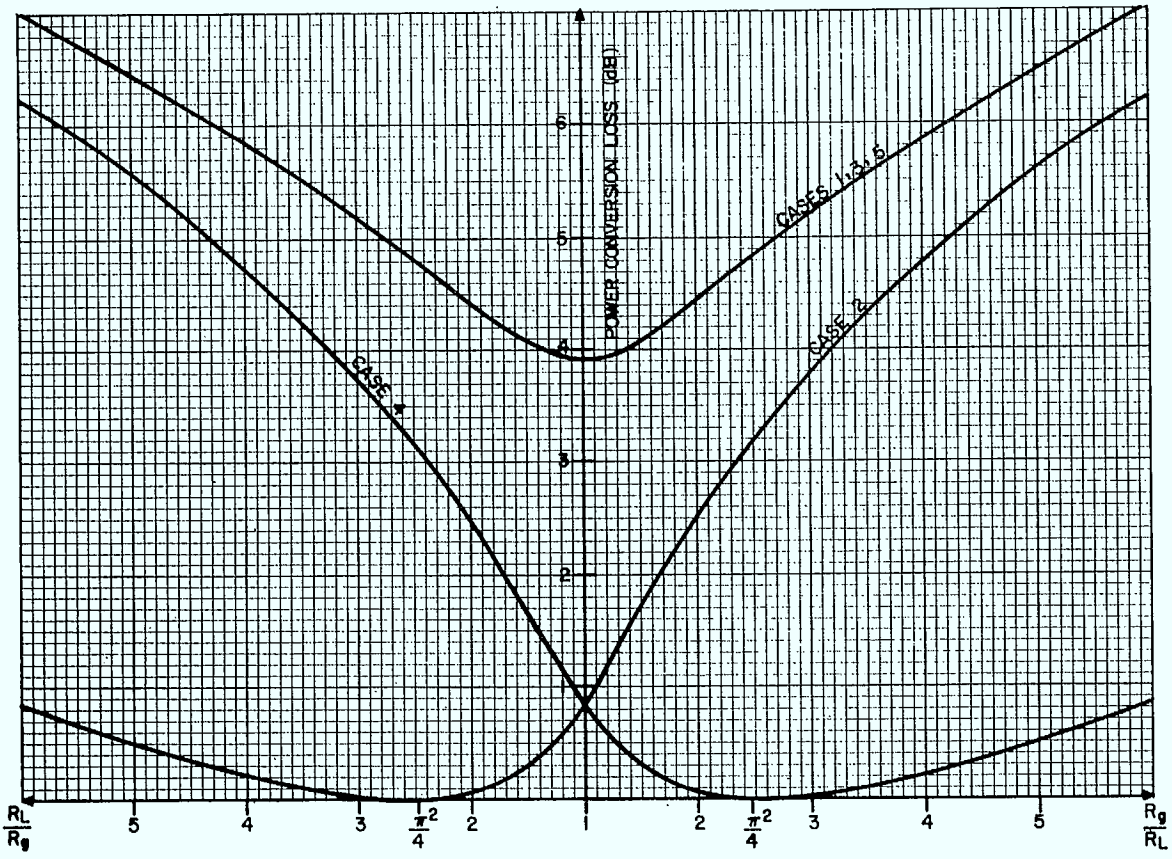

Fig. A-1. Variation of the conversion loss of diode ring mixers with load resistance when terminated in frequency selective (resistive or zero or infinite) impedances.

APPENDIX B

Conversion Loss of Reactively Terminated Mixers

The two cases of reactively terminated mixers illustrated in Figure B-1 will be considered here. In the following analysis, it will be assumed that the output tuned circuits maintain sufficient loaded Q for their impedances to be considered to be zero or infinite at unwanted sidebands. Furthermore, it will also be assumed that the output impedance Z_1 of the input filter (when terminated at its input by R_g) is totally reactive at all unwanted frequencies and equal to the source impedance R_g at the signal frequency.

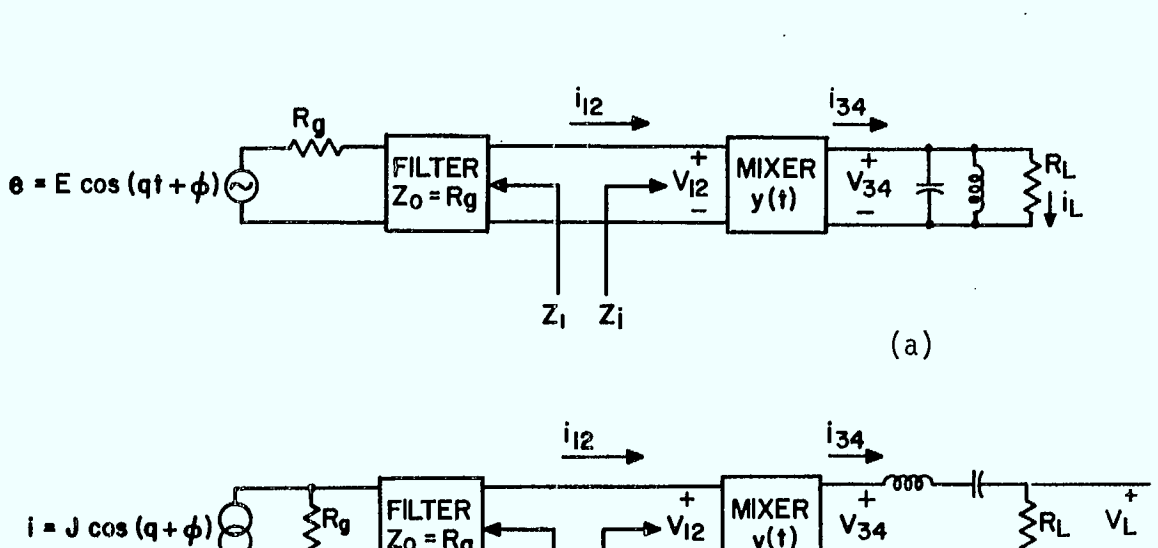

Fig. B-1. Two cases of reactively terminated mixer systems to be analyzed
(a) parallel tuned output
(b) series tuned output.

Case 1. Output Voltage Tuned to p-q

Since the output voltage v_{34} is tuned to p-q, the output voltage waveform is sinusoidal and may therefore be written

$$v_{34} = V \cos(p-q)t. \qquad \ldots\ldots (26)$$

$$v_{12} = y(t)v_{34}$$

$$= \frac{2}{\pi} V[\cos qt + \cos(2p-q)t - \frac{1}{3}\cos(2p+q) - \frac{1}{3}\cos(4p-q)t + \ldots] \quad \ldots\ldots(27)$$

The input current is then given by

$$i_{12} = \frac{E\cos(q+\phi) - \frac{2}{\pi}V\cos qt}{R_g} - \frac{2}{\pi}V[\frac{1}{X_{2-}}\sin(2p-q)t - \frac{1}{3X_{2+}}\sin(2p+q)t$$

$$- \frac{1}{3X_{4-}}\sin(4p-q)t + \frac{1}{5X_{4+}}\sin(4p+q)t + \ldots] * \quad \ldots\ldots(28)$$

where ϕ is an arbitrary phase angle which represents the phase difference between the source voltage and the voltage v_{12} at frequency q, and $X_{n\pm}$ is the reactance of Z_1 at $np\pm q$. The output current i_{34} corresponding to i_{12} is then given by

$$i_{34} = y(t)i_{12}$$

$$= \frac{2}{\pi}\frac{E}{R_g}[\cos((p+q)t+\phi) + \cos((p-q)t-\phi) - \frac{1}{3}\cos((3p+q)t+\phi) - \frac{1}{3}\cos((3p-q)t-\phi) + \ldots]$$

$$- \frac{4}{\pi^2}\frac{V}{R_g}[\cos(p-q)t + \cos(p+q)t - \frac{1}{3}\cos(3p+q)t - \frac{1}{3}\cos(3p-q)t + \ldots]$$

$$- \frac{4}{\pi^2}\frac{V}{X_{2-}}[\sin(3p-q)t + \sin(p-q)t - \frac{1}{3}\sin(5p-q)t + \frac{1}{3}\sin(p+q)t + \frac{1}{5}\ldots]$$

$$- \frac{4}{\pi^2}\frac{V}{S_{2+}}[-\frac{1}{3}\sin(3p+q)t + \frac{1}{3}\sin(p+q)t + \frac{1}{9}\sin(5p+q)t - \frac{1}{9}\sin(p-q)t - \frac{1}{15}\ldots]$$

$$- \frac{4}{\pi^2}\frac{V}{X_{4-}}[-\frac{1}{3}\sin(5p-q)t - \frac{1}{3}\sin(3p-q)t + \frac{1}{9}\sin(p-q)t + \frac{1}{9}\sin(7p-q)t - \frac{1}{15}\ldots]$$

etc. $\quad \ldots\ldots(29)$

The only current in the load resistance is at (p-q). Therefore, collecting all (p-q) terms in (29) gives the load current,

$$i_L = \frac{V}{R_L}\cos(p-q)t = \frac{1}{R_g}[\frac{2}{\pi}E\cos((p-q)t-\phi) - \frac{4}{\pi^2}V\cos(p-q)t]$$

$$- \frac{4}{\pi^2}V[\frac{1}{X_{2-}} - \frac{1}{9X_{2+}} + \frac{1}{9X_{4-}} - \frac{1}{25X_{4+}} + \ldots]\sin(p-q)t$$

$$= [\frac{2}{\pi}\frac{E}{R_g}\cos\phi - \frac{4}{\pi^2}\frac{V}{R_g}]\cos(p-q)t + [\frac{2}{\pi}\frac{E}{R_g}\sin\phi - \frac{4}{\pi^2}\frac{V}{X_{eq}}]\sin(p-q)t \quad \ldots\ldots(30)$$

* The sine terms occur here as a result of the 90° phase relationship between the current and voltage at all frequencies $np\pm q$ in the stopband of the filter.

where

$$\frac{1}{X_{eq}} \triangleq \frac{1}{X_{2-}} - \frac{1}{9X_{2+}} + \frac{1}{9X_{4-}} - \frac{1}{25X_{4+}} + \ldots$$

To satisfy the equality, the coefficient of sin(p-q)t must be zero. Therefore

$$\sin\phi = \frac{\pi}{2}\frac{R_g}{E} \times \frac{4}{\pi^2}\frac{V}{X_{eq}} = \frac{2}{\pi}\left(\frac{V}{E}\right)\frac{R_g}{X_{eq}} . \qquad \ldots\ldots (31)$$

Equating the coefficients of cos(p-q)t in (30) and solving for the voltage conversion loss yields

$$\frac{E}{V} = \frac{1}{\cos\phi}\left(\frac{\pi}{2}\frac{R_g}{R_L} + \frac{2}{\pi}\right) \qquad \ldots\ldots (32)$$

Combining (31) and (32) and solving for $\tan\phi$ yields

$$\tan\phi = \frac{4}{\pi^2}\frac{R_g}{X_{eq}}\frac{1}{\left(\frac{R_g}{R_L} + \frac{4}{\pi^2}\right)} . \qquad \ldots\ldots (33)$$

Using (33) to substitute for $\cos\phi$ in equation (32) yields, after simplifying

$$\left(\frac{E}{V}\right) = \left[\left(\frac{\pi}{2}\frac{R_g}{R_L} + \frac{2}{\pi}\right)^2 + \frac{4}{\pi^2}\frac{R_g^2}{X_{eq}^2}\right]^{1/2} . \qquad \ldots\ldots (34)$$

The power conversion loss L therefore becomes

$$L = \left(\frac{E}{V}\right)^2 \frac{R_L}{4R_g}$$

$$= \frac{R_L}{4R_g}\left[\left(\frac{\pi}{2}\frac{R_g}{R_L} + \frac{2}{\pi}\right)^2 + \frac{4}{\pi^2}\frac{R_g^2}{X_{eq}^2}\right] . \qquad \ldots\ldots (35)$$

From this equation, it may be seen that for low conversion loss, X_{eq} must be large or, equivalently, the sum $\frac{1}{X_{2-}} - \frac{1}{9X_{2+}} + \frac{1}{9X_{4-}} - \frac{1}{25X_{4+}} + \ldots$ must be small. This condition may be approached in practice if the filter output impedance is inductive in the stopband since then, the terms $X_{n\pm}$ will be monotonically increasing with n.

The input impedance Z_i is defined as the ratio of the complex input voltage at frequency q to the complex input current at frequency q. From (27)

$$v_{12} = \frac{2}{\pi} V\cos qt = R_e\left[\frac{2}{\pi} V e^{jqt}\right] . \qquad \ldots\ldots (36)$$

From (28)

$$i_{12} = \frac{1}{R_g}\left[E\cos(qt+\phi) - \frac{2}{\pi} V\cos qt\right]$$

which, after expanding $\cos(qt+\phi)$ and substituting for $\cos\phi$ and $\sin\phi$ from (31) and (32), reduces to

$$i_{12} = \frac{V}{R_L}\frac{\pi}{2}\cos qt - \frac{V}{X_{eq}}\frac{2}{\pi}\sin qt$$

$$= \sqrt{\frac{\pi^2}{4R_L^2} + \frac{4}{\pi^2 X_{eq}^2}}\; V \,\mathrm{Re}\left[e^{j(qt+\theta)}\right] \qquad \ldots\ldots (37)$$

where

$$\theta = \tan^{-1}\left(\frac{4}{\pi^2}\frac{R_L}{X_{eq}}\right)$$

The input impedance Z_i is therefore given by

$$Z_i = \frac{\frac{2}{\pi}}{\sqrt{\frac{\pi^2}{4R_L^2} + \frac{4}{\pi^2 X_{eq}^2}}} \angle -\theta$$

$$= \frac{4}{\pi^2} R_L \frac{1}{\sqrt{1 + \frac{16 R_L^2}{\pi^4 X_{eq}^2}}} \angle -\theta \qquad \ldots\ldots (38)$$

Case 2. Output Current Tuned to p-q

The analysis in this case (Fig. B-1(b)) is very similar to that for Case 1 above. However, in this case the output current is sinusoidal and may be written

$$i_{34} = I\cos(p-q)t.$$

This current, transformed by the modulating function corresponds to an input voltage v_{12} given by

$$v_{12} = R_g[J\cos(qt+\theta) - \frac{2}{\pi} I\cos qt] - \frac{2}{\pi} I[X_{2-}\sin(2p-q)t - \frac{1}{3}X_{2+}\sin(2p+q)t$$

$$- \frac{1}{3}X_{4-}\sin(4p-q)t + \frac{1}{5}X_{4+}\sin(4p+q)t + \ldots]. \qquad \ldots\ldots (39)$$

Transforming this voltage by y(t) and collecting all terms at frequency p-q gives the voltage across the load resistance,

$$V_L = I R_L \cos(p-q)t = R_g[\frac{2}{\pi} J\cos((p-q)t-\phi) - \frac{4}{\pi^2} I\cos(p-q)t]$$

$$- \frac{4}{\pi^2} I[X_{2-} - \frac{1}{9}X_{2+} + \frac{1}{9}X_{4-} - \frac{1}{25}X_{4+} + \ldots]\sin(p-q)t$$

$$= \left[\frac{2}{\pi} J R_g \cos\phi - \frac{4}{\pi^2} IR_g\right] \cos(p-q)t + \left[\frac{2}{\pi} JR_g \sin\phi - \frac{4}{\pi^2} IX_{eq}\right] \sin(p-q)t \quad \ldots\ldots (40)$$

where, in this case, $X_{eq} \triangleq X_{2-} - \frac{1}{9}X_{2+} + \frac{1}{9}X_{4-} - \frac{1}{25}X_{4+} + \ldots$.

Equating coefficients in (40) and solving for ϕ and (J/I) as in section 1 yields the power conversion loss

$$L = \frac{R_g}{4R_L}\left[\left(\frac{\pi}{2}\frac{R_L}{R_g} + \frac{2}{\pi}\right)^2 + \frac{4}{\pi^2}\frac{X_{eq}^2}{R_g}\right] \quad \ldots\ldots (41)$$

From this equation, it may be seen that, in this case, for low conversion loss, $X_{eq} = X_{2-} - \frac{1}{9}X_{2+} + \frac{1}{9}X_{4-} - \frac{1}{25}X_{4+} + \ldots$ must be small. This condition may be approached in practice if the filter output impedance is capacitive in the stopband since then, the magnitudes ($X_{n\pm}$ is negative for capacitances) of the terms $X_{n\pm}$ will be monotonically decreasing.

The input impedance may again be determined in a manner similar to that for Case 1.

LIST OF SYMBOLS

p = angular frequency of local oscillator

q = angular frequency of signal source

$np \pm q$ = sideband frequency components

n, m = integers

$y(t)$ = modulating function

r_d = diode dynamic on resistance

Z_s = effective source impedance

Z_L = effective load impedance

R_s, R_L = resistive portions of Z_s and Z_L

R_g = generator output resistance

R_p = external load resistance

Z_i = complex input impedance of modulator measured at input terminals of modulator at frequency Q

R_i = resistive component of Z_i

Z_1 = complex output impedance of input filter as observed by the modulator

$X_{n\pm}$ = reactance of Z_1 at frequency $np \pm q$

v_{12}, i_{12} = instantaneous voltage and current at the modulator input

v_{34}, i_{34} = instantaneous voltage and current at the modulator output

v_L, i_L = instantaneous load voltage and load current

E = peak open circuit output voltage of the signal generator

J = peak current of Norton equivalent current source

V = modulator peak output voltage at frequency $p-q$

I = modulator peak output current at frequency $p-q$

L = conversion loss defined as the ratio of the maximum available power from the source to the power delivered to the load at the desired output frequency